ELSEVIER

Contents lists available at ScienceDirect

Cleaner Environmental Systems

journal homepage: www.journals.elsevier.com/cleaner-environmental-systems



Economic and life cycle assessment of novel hybrid energy and fuel generation systems from municipal waste through plasma gasification and anaerobic digestion coupled with carbon capture and storage

Qurrotin Ayunina Maulida Okta Arifianti ^{a,b,*}, Maria Fernanda Rojas Michaga ^a, Karim Rabea ^{a,c}, Stavros Michailos ^d, Kevin J. Hughes ^a, Lin Ma ^a, Derek Ingham ^a, Mohamed Pourkashanian ^a

- a Energy 2050, School of Mechanical, Aerospace and Civil Engineering, The University of Sheffield, Sheffield, S3 7RD, United Kingdom
- ^b Universitas Internasional Semen Indonesia, Gresik, East Java, Indonesia
- ^c Department of Mechanical Power Engineering, University of Tanta, Egypt
- ^d School of Engineering, University of Hull, Hull, HU6 7RX, United Kingdom

ARTICLE INFO

Keywords: Novel system design Sustainable waste management Waste-to-energy

Plasma gasification Carbon capture and storage Economic analysis LCA

ABSTRACT

Achieving climate goals demands novel system designs that enable the conversion of municipal waste, such as plastic and food waste into energy and fuels with minimal environmental impact. This study proposes an innovative multi-energy generation system that integrates plasma gasification for plastic waste and anaerobic digestion for food waste, coupled with carbon capture and storage (CCS) technologies. This novel conceptual design aims to maximize energy recovery while reducing lifecycle emissions compared to conventional waste-toenergy (WtE) pathways. Two novel system configurations were assessed: (1) a combined cooling, heating, and power (CCHP) system, and (2) a CCHP system integrated with liquid biomethane production. Each configuration was evaluated under three CCS strategies: no CCS, pre-combustion CCS, and post-combustion CCS. The economic analysis and life cycle assessment (LCA) highlight the economic and environmental trade-offs of each design. Specifically, in Scenario 1, the levelized cost of electricity (LCOE) increases from 0.171 USD/kWh (no CCS) to 0.311 and 0.354 USD/kWh while in Scenario 2, the levelized cost of biomethane (LCObM) rises from 0.176 USD/ kWh to 0.314 and 0.374 USD/kWh for pre- and post-combustion CCS, respectively. While CCS raises production costs, they also represent a tangible commitment to reducing emissions and underscore that transitioning to cleaner energy systems often entails higher near-term expenditures. Across both scenarios, the levelized cost of waste treatment (LCOWT) spans 0.081-0.236 USD/kg of waste. Global warming potential (GWP) ranges from -0.191 to 0.662 kgCO₂-eq/kg of feedstock for Scenario 1, and 0.123 to 0.746 kgCO₂-eq/kg for Scenario 2. This work provides the first integrated assessment of such a hybrid WtE system, offering new insights for sustainable waste valorisation. The proposed novel designs support future detailed engineering studies and inform policymaking for low-carbon waste management.

Nomenclature

(continued on next column)

(continued)

^{*} Corresponding author. Energy 2050, School of Mechanical, Aerospace and Civil Engineering, The University of Sheffield, Sheffield, S3 7RD, United Kingdom. E-mail address: qamarifianti1@sheffield.ac.uk (Q.A.M.O. Arifianti).

(continued)

(continuea)	
IP ₂	capacity proportion required for the equivalent process in the observed
	system
k	scaling factor in the six-tenths factor rule
N_{np}	quantity of non-particulate processing stages
N_{OL}	quantity of operators assigned to each shift
P	quantity of processing stages
P_n	gross profits
t	tax rate
S	actual capacity
S_0	base capacity
\$	price
\dot{W}_{elec}	net electricity
Acronyms	
AD	anaerobic digester
ARC	absorption refrigeration cooler
BL	blowdown loss
CAPEX	capital expenditure
CC	combustion chamber
CCGT	combined cycle gas turbine
CI	confidence interval
CHP	combined heating and power
CCHP	combined cooling, heating, and power
CCS	carbon capture storage
CEPCI	chemical engineering plant cost index
COC	cycles of concentration
COP	coefficient of performance
DCFA	discounted cash flow analysis
DGO	direct and general overhead
DL	drift loss
EL	evaporation loss
FCI	fixed capital investment
FOM	fixed operating, and maintenance costs
GHSV	gas hourly space velocity
GT	gas turbine
GWP	global warming potential
HP	high-pressure
HPWS	high pressure water scrubber
HRSG	heat recovery steam generator
HTWGSR	high temperature water gas shift reactor Indirect cost
IC IDC	installed direct costs
IDC IP	intermediate-pressure
IRR	internal rate of return
ITF WC	insurance, tax and financing working capital
LCA	life cycle assessment
LCI	life cycle inventory
LCIA	life cycle impact assessment
LCOE	levelized cost of electricity
LCObM	levelized cost of liquid biomethane
LCOWT	levelized cost of waste treated
LHV	lower heating value
LNG	liquid natural gas
LP	low-pressure
LS	labour and supervision
LTWGSR	low temperature water gas shift reactor
MEA	monoethanolamine
ML	methane liquefier
MLM	maintenance labour and materials
MSW	municipal solid waste
MW	megawatt
NIDC	non-installed direct costs
NPV	net present value
OPEX	operating expenditure
PEC	purchased equipment cost
PG	plasma gasifier
ST	steam turbine
TCR	total capital requirement
TDC	total direct costs
T&S	transportation and storage
VC	variable cost
WC WF	working capital water footprint
WGS	water footprint water gas shift
WGS WGSR	water gas shift reactor
WtE	water gas sinit reactor waste-to-energy
wt	waste-to-energy weight
VV L	weight

1. Introduction

Effective waste management has become a key target for achieving sustainability of cities and human settlements, as emphasized in Target 11 of the United Nations Sustainable Development Goals (United Nations: Department of Economic and Social Affairs, 2023). Among various types of waste, plastic and food waste are the most dominant in almost all countries (Brahme et al., 2023). Mismanagement of plastic and food waste can have severe negative impacts on the environment. Plastic waste is particularly problematic due to its resistance to natural decomposition. Over time, it can break down into tiny particles, entering waterways and harming aquatic ecosystems (Lebreton and Andrady, 2019). Similarly, untreated food waste can decompose and release methane as a potent greenhouse gas into the atmosphere, which can contribute to climate change (Wei et al., 2024). The increasing population exacerbates the issue, leading to higher waste generation. Projections indicate that global waste generation will reach 2.68 billion metric tonnes by 2030 (United Nations Environment Programme and International Solid Waste Association, 2024). These pressing issues necessitate immediate action to minimize waste and develop novel methods to convert waste into valuable products.

One effective strategy for addressing these challenges is WtE conversion, which transforms waste into useable energy, depending on the type of waste and its calorific value. Among the WTE technologies, incineration is widely used; however, it poses challenges such as greenhouse gas emissions and air pollution (United Nations Environment Programme and International Solid Waste Association, 2024). An alternative thermal treatment technology is plasma gasification, which offers a cleaner approach to WtE conversion (Mountouris et al., 2006).

Plasma gasification operates at extremely high temperatures, with the feedstock exposed to plasma generated by an external heating source reaching approximately 4000 °C (Minutillo et al., (Montiel-Bohórquez et al., 2021). This extreme heat enables the complete breakdown of almost any type of feedstock, whether hazardous or non-hazardous, into simpler components (Akbarian et al., 2022). It decomposes tar, char, and dioxins, and melts tar and ash into a glassy slag, a non-leachable by-product with potential applications in construction (Jones et al., 2013). The high operating temperature greatly reduces these impurities, resulting in cleaner syngas (Mountouris et al., 2006). The low tar content in plasma-derived syngas broadens its potential applications, enabling advanced conversion processes such as hydrogen purification, Fischer-Tropsch synthesis, and methanol production, which are often sensitive to tar and other contaminants (Oliveira et al., 2022). In contrast, conventional gasification operates at much lower temperatures (400-850 °C), which are insufficient to fully decompose feedstock. As a result, conventional gasifiers typically produce syngas with higher tar and impurity levels, necessitating extensive downstream cleaning (Mountouris et al., 2006). It also delivers higher energy performance, with electricity generation efficiencies reaching 51 % compared to 20 % for RDF incineration plants (Oliveira et al., 2022).

Despite these advantages, current limitations include high plasma torch energy demand, substantial capital investment for industrial-scale facilities, and accelerated electrode wear under extreme conditions (Janajreh et al., 2013), (Rutberg et al., 2011), (Fridman, 2008), (Zhou et al., 2023). However, ongoing advances in reactor design, plasma torch efficiency, and high-durability materials are steadily reducing these challenges, strengthening its economic viability and operational reliability (Nagar and Kaushal, 2024). In this study, mixed plastic waste is utilized as feedstock in plasma gasification. Previous research has extensively explored the use of plastic waste in plasma gasification (Xu et al., 2025), (Rutberg et al., 2013), (Cho et al., 2015), (Mallick and Vairakannu, 2023), (Cudjoe and Zhu, 2024), (Galaly and Dawood, 2023), (Rida Galaly et al., 2024), (Gabbar et al., 2020), (Cudjoe and Wang, 2022), (Zhao et al., 2023), (Mallick and Prabu, 2022), (Chari et al., 2023), with studies reporting its conversion into various products such as syngas (Rutberg et al., 2013), (Cho et al., 2015), (Mallick and

Vairakannu, 2023), (Cudjoe and Zhu, 2024), pyrolysis oil (Galaly and Dawood, 2023), (Rida Galaly et al., 2024), electricity (Gabbar et al., 2020), (Cudjoe and Wang, 2022), hydrogen (Zhao et al., 2023), hydrogen and electricity (Mallick and Prabu, 2022), (Chari et al., 2023), and methanol and electricity (Xu et al., 2025). While these studies demonstrate the versatility of plasma gasification, they predominantly focus on producing a single output. This highlights a research gap in exploring multi-output systems, which have the potential to offer significant benefits. Multi-output systems can improve energy efficiency, reduce fuel consumption, and lower greenhouse gas emissions, making them a promising innovation for sustainable WtE conversion (Soltani, 2019), (Zare, 2020), (Jouhara et al., 2018).

This study not only investigates the utilization of plastic waste but also examines the potential of converting food waste into energy. By focusing on the plastic and food wastes, the research targets two of the most significant waste streams in terms of volume and environmental impact. However, the high moisture content of food waste, ranging from 70 % to 90 %, makes it unsuitable for gasification (Zhang et al., 2007), which requires feedstock with a moisture content of 30 % or less (Zhang et al., 2020). Anaerobic digestion presents a suitable solution as microorganisms can effectively process high-moisture food waste to produce biogas (Xu et al., 2018), (Antoniou et al., 2019). Combining plasma gasification of plastic waste with anaerobic digestion of food waste in an energy system could enhance resource efficiency. Nonetheless, to the best of the authors' knowledge, no previous study has proposed a novel system design that integrates plasma gasification and anaerobic digestion for diverse energy production, such as CCHP and liquid biomethane.

Decarbonizing WtE power plants are crucial for achieving the climate targets set by the International Energy Agency (International Energy Agency, 2023) and the Intergovernmental Panel on Climate Change (Calvin et al., et al., 2023). Although plastic waste plasma gasification offers considerable potential for energy recovery, its integration with carbon capture and storage (CCS) systems has been scarcely investigated. To date, only two studies have explored this integration: one employed a monoethanolamine (MEA)-based post-combustion CCS system with a 90 % carbon capture rate (Mallick and Prabu, 2022), while the other examined an MEA-based pre-combustion CCS system with the same capture rate (Chari et al., 2023). This limited research highlights a significant knowledge gap regarding CCS integration in plastic waste plasma gasification. Further investigations are required to assess the feasibility, performance, and environmental implications of CCS deployment in this context. Moreover, existing studies have only examined individual CCS configurations (either pre- or post-combustion CCS) which limits insights into their comparative effectiveness. Consequently, a comprehensive study that evaluates both pre- and post-combustion CCS integration within a single system is essential for identifying the most efficient approach. Additionally, both studies adopted a 90 % carbon capture rate, despite recent advancements enabling capture efficiencies of up to 95 %. Evaluating CCS performance at a 95 % capture fraction is important to minimize residual emissions and provide deep decarbonisation of WtE systems.

The authors have previously examined the technical performance of a multi-energy output generation system that integrates plastic waste plasma gasification and food waste anaerobic digestion with CCS (Arifianti et al., 2025). However, to comprehensively assess the system's feasibility, a detailed economic analysis and LCA are essential. These evaluations are crucial for determining the system's economic viability, confirming its potential to reduce carbon emissions, and providing valuable insights for policymakers.

Despite their importance, comprehensive evaluations that combine economic analysis and LCA remain limited in the existing literature which highlights a significant knowledge gap. To address this, the current study builds on the established technical data to present a detailed economic analysis and LCA investigation for the production of multiple energy outputs across various scenarios and process configurations. The

analysis considers two scenarios: one focusing on CCHP production, and another involving both CCHP and liquid biomethane production. Each scenario includes three cases: a baseline case without CCS integration, a case with a pre-combustion CCS system (referred to as "w/pre-CCS"), and a case with a post-combustion CCS system (referred to as "w/post-CCS"). The results from this study contribute to advancing the understanding of innovative, low-emission system designs for WtE applications.

2. Methodology

2.1. System description

Feedstock is sourced from the 37-ha Benowo landfill in Surabaya, Indonesia's second-largest city. The system processes mixed waste, approximately 74 wt % food waste and 26 wt % plastic, at feed rates of 13 kg/s (46 MW $_{th}$) for food waste and 5 kg/s (184 MW $_{th}$) for plastic, respectively. The WtE system was designed to generate multiple valuable outputs, including electricity, cooling, heating, and liquid fuel, while also meeting the internal heat and electricity demands for system operation. Additionally, the system generates useful by-products, such as slag from plasma gasification, which can be repurposed as construction material, and digestate from anaerobic digestion, which can be used as fertilizer.

The entire process was modeled in Aspen Plus (see (Arifianti et al., 2025) for full technical details). Mixed plastic waste, chosen for its low moisture content, is first crushed and fed into a plasma gasifier operating at 2500 °C, with air and steam as gasifying agents. A plasma torch heats the incoming air to 4000 °C, supplying the thermal energy required; this torch is powered by electricity generated on-site. The raw syngas leaving the gasifier has a molar composition of 42.6 % $\rm H_2$, 24 % $\rm CO$, 1.4 % $\rm CO_2$ while slag is produced at a rate of 0.66 kg/s.

Food waste, by contrast, contains 76 % moisture and is thus routed to a mesophilic anaerobic digester at 38 °C, producing biogas composed of 47.5 % CH₄ and 43.4 % CO₂ (molar) and generates digestate "fertilizer" at 15.95 kg/s. In the baseline case, the heating demand required to maintain the operating temperature of the AD process is met by recovering heat from the raw syngas and the flue gas. In contrast, for the scenario incorporating CCS, the heating requirement is fulfilled by utilizing heat recovered from the vapor stream exiting the stripper in the CCS plant, prior to the reflux condenser.

Two scenarios are explored in this study. In Scenario 1, syngas and biogas are utilized as fuels in the combined cycle gas turbine (CCGT) to generate electricity, as illustrated in Fig. 1. The heat recovered from the flue gas of the CCGT is then used in an absorption refrigeration cooler (ARC) to provide residential cooling, while the remaining waste heat is applied to fish drying industries. Scenario 1 is referred to as a CCHP production system. Meanwhile, in Scenario 2, only syngas is used as fuel in the CCGT, while the biogas is converted into liquid biomethane through a water scrubber (WS) and methane liquefier (ML), as shown in Fig. 2. Scenario 2 is referred to as a CCHP and liquid biomethane production system. Both Figs. 1 and 2 outline the system boundaries for the economic analysis and LCA conducted in this study.

Each scenario includes three cases: a baseline case without CCS integration, a case integrated with pre-combustion CCS (w/pre-CCS), and a case integrated with post-combustion CCS (w/post-CCS). In the w/pre-CCS case, a WGSR is installed after the PG, and the CCS plant is positioned between the WGSR and the CCGT. To facilitate the WGSR reaction, 10 % of the raw syngas is extracted and burned to generate steam for the process. The water gas shift (WGS) process is carried out in two stages to maximize CO conversion: first, at 450 °C in a high-temperature WGSR (HTWGSR) using a Fe–Cr catalyst, and second, at 200 °C in a low-temperature WGSR (LTWGSR) employing a CuO/ZnO/Al₂O₃ catalyst. To lower the temperature of the stream between the HTWGSR and LTWGSR, as well as the stream exiting the LTWGSR prior to entering the CCS plant, heat is recovered and used to generate low-

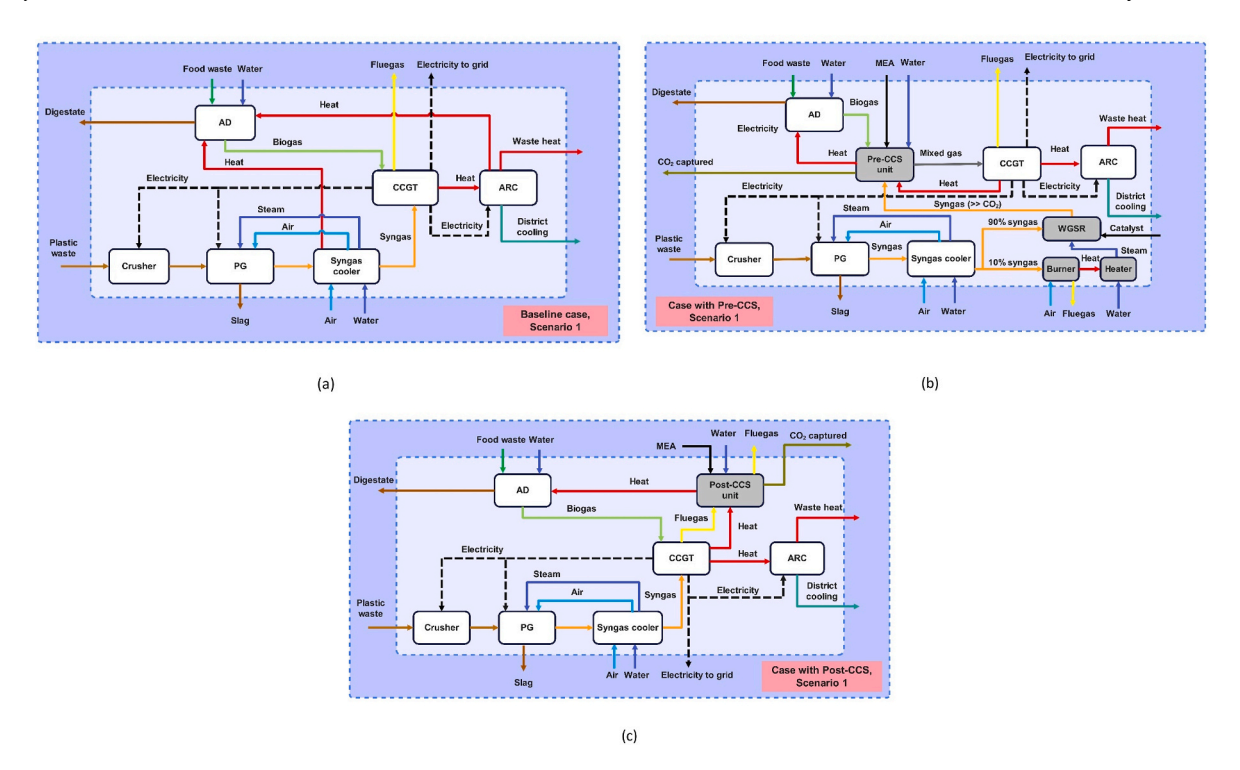


Fig. 1. System boundaries and configurations for Scenario 1 (products: CCHP) with three different cases: (a) baseline, (b) w/pre-CCS, (c) w/post CCS.

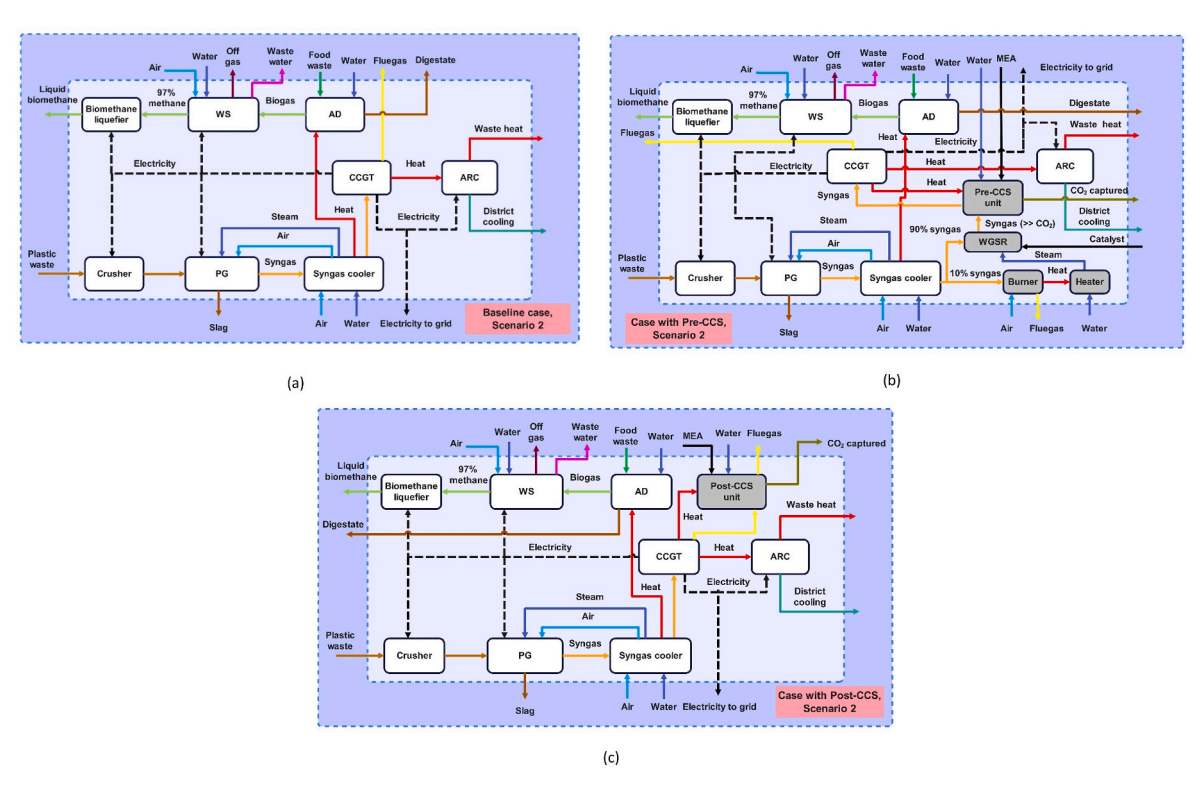


Fig. 2. System boundaries and configurations for Scenario 2 (products: CCHP, and liquid fuel) with three different cases: (a) baseline, (b) w/pre-CCS, (c) w/post CCS.

pressure (LP) steam, which can subsequently be utilized for heating the stripper in the CCS system.

The syngas exiting the WGSR, now enriched with $\rm CO_2$, is directed to the pre-CCS plant, where $\rm CO_2$ is captured at a rate of 95 %. In Scenario 1, the syngas is first blended with biogas before entering the CCS plant, whereas in Scenario 2, only syngas is used as the input stream. The chemical solvent employed is MEA at a concentration of 35 wt%. The

CCS plant comprises two main components: an absorber and a stripper. The feed gas enters at the bottom of the absorber column, where it is contacted counter currently with the MEA solution sprayed from the top. The column packing is designed to operate below the 80 % flooding limit to ensure stable and efficient mass transfer. Within the absorber, $\rm CO_2$ is absorbed into the MEA, forming a $\rm CO_2$ -rich solvent, while the cleaned gas exits at the top. The $\rm CO_2$ -rich solvent is then directed to the stripper,

where it is heated using LP steam generated within the system to release the absorbed CO_2 . Once the CO_2 is removed, the regenerated lean solvent is recycled back to the absorber. The CO_2 stream exiting the stripper is cooled to condense water and separate vapor components. The purified CO_2 is then compressed to supercritical conditions and further cooled to a liquid state for transport and storage in deep geological formations.

Afterwards, the clean gas, containing minimal CO_2 , is used as fuel in the CCGT. In the gas turbine (GT) cycle, the required air flow rate for combustion is determined to ensure the turbine exhaust reaches 1350 °C. This high-temperature exhaust gas drives the gas turbine to generate electricity. The residual thermal energy in the exhaust is then recovered in the heat recovery steam generator (HRSG) of the steam turbine (ST) cycle. To maximize power output, the steam cycle operates with three pressure levels: high-pressure (HP), intermediate-pressure (IP), and LP steam. The LP steam is split into two streams: one directed to the LP turbine, and the other supplied to the CCS plant to meet the reboiler heat duty in the stripper. After passing through the HRSG, the exhaust gas flows into the ARC for further heat recovery.

In the ARC, the working fluid is a mixture of lithium bromide and water (LiBr-H $_2$ O). Lithium bromide serves as the absorbent, enabling water to evaporate at low temperatures by maintaining low system pressure. The primary components of the system include the evaporator, absorber, generator, condenser, throttling devices, and a solution pump. Waste heat from the exhaust gas is utilized in the generator, where it heats the working fluid, causing the separation of water vapor from the LiBr solution. The water vapor then flows to the condenser, where it is cooled and condensed into liquid water. This liquid refrigerant is throttled and directed to the evaporator, where it absorbs heat from the surroundings, producing the cooling effect. The resulting water vapor is drawn into the absorber and absorbed by the concentrated LiBr solution, forming a dilute solution that is pumped back to the generator to complete the cycle. The residual heat in the flue gas exiting the ARC is subsequently used as a thermal source for fish drying in local industries.

In the w/post-CCS case, the CCS plant is positioned downstream of the ARC to recover waste heat from the CCGT flue gas. The cooled flue gas is then directed to the post-CCS plant, where CO₂ is captured before the remaining gas is released into the atmosphere. The overall process in the post-CCS plant closely resembles that of the w/pre-CCS case, but with a few notable distinctions. First, the absorber column in the post-CCS configuration features a larger packing diameter to accommodate the higher volumetric flow rate of flue gas, which helps prevent flooding and ensures effective mass transfer. Second, the lean and rich solvent loadings in the post-CCS system are slightly lower than in the pre-CCS system, reflecting the lower CO₂ concentration in the flue gas compared to the gas streams in Scenario 1 (mixed syngas and biogas) and Scenario 2 (syngas only). For clarity, components that are unique to the w/pre-CCS and w/post-CCS configurations are highlighted using grey blocks in the system diagrams.

In Scenario 2, where biogas is upgraded to liquid biomethane, a water scrubber and a methane liquefaction system are employed. The water scrubber operates under high pressure and low temperature conditions to enhance the solubility of CO_2 in water, thereby improving CO_2 removal efficiency. The main components of the water scrubbing system include compressors, absorbers, strippers, pumps, and heat exchangers. After treatment in the scrubber, the methane concentration in the biogas can reach up to 97.7 %. The upgraded biogas is then directed to a multistage compressor, where its pressure is increased to 200 bar in preparation for liquefaction. In the liquefaction stage, the HP gas is cooled and subsequently expanded to achieve the low temperatures necessary for methane condensation and liquefaction. The flow diagram and operating conditions of each component used in both scenarios are provided in reference (Arifianti et al., 2025).

2.2. Technical details

Table 1 summarizes the process model results, including energy generation, CO_2 capture, and overall system efficiency, based on the authors' previous work (Arifianti et al., 2025). Detailed operating conditions for all components are provided in **Supplementary Information Section S.1.** The process efficiencies in this study are calculated based on detailed energy and exergy balances, following the methodology described in (Arifianti et al., 2025). The total energy input consists of the chemical energy contained in the feedstock: mixed plastic waste and food waste. Specifically, the energy content of the plastic waste and food waste feedstocks is quantified using their lower heating values and mass flow rates.

The useful energy outputs include electricity generated by the CCGT, thermal energy in the form of heating and cooling delivered by the ARC and other heat recovery systems, and, in Scenario 2, liquid biomethane produced from upgraded biogas. Energy efficiency is calculated as the ratio of the sum of all useful energy outputs (CCHP, and liquid fuel) to the total energy input from the feedstocks. Exergy efficiency considers the quality and work potential of the energy inputs and outputs by comparing the chemical exergy of the feedstock inputs to the exergy of the useful energy products.

These technical data form the foundation for the economic and life cycle assessments presented in subsequent sections. The results provide a comprehensive overview of system performance across different scenarios and configurations, highlighting key metrics such as energy output, carbon capture rates, and conversion efficiencies. The following sections offer a detailed analysis of these technical aspects to support the ensuing economic and environmental evaluations.

2.3. Economic evaluation

The primary objective of the economic evaluation is to determine the levelized cost of electricity (LCOE) for each case in Scenario 1, where electricity is the main product, while cooling and heating are the coproducts and the levelized cost of liquid biomethane (LCObM) for each case in Scenario 2, where liquid biomethane is the main product. Additionally, the levelized cost of waste treated (LCOWT) is determined for each case in both scenarios. A discounted cash flow analysis (DCFA) is performed to calculate these costs for net present value (NPV) = 0 or for an internal rate of return (IRR) = discount rate (i_d) based on various financial assumptions detailed in Table 2. The basis of the DCFA model is defined by the equation:

$$\sum_{n=1}^{n=20} \frac{CF_n}{(1+IRR)^n} = 0$$
 (Eq. 1)

$$CF_n = P_n(1-t) + D_n t \tag{Eq. 2}$$

where CF_n represents the after-tax cash flow for each year, n is the number of years, P_n denotes gross profits, t is the tax rate, and D_n refers to the depreciation of plant assets, assumed to occur over 10 years of operation.

Gross profit is calculated by monetizing the useful energy outputs of the system, which include electricity, cooling, heating, and liquid biomethane. For electricity, cooling, and heating, the exergy content is used to capture the quality and usefulness of these energy forms, reflecting their economic value more accurately than raw energy content. However, for liquid biomethane, the calculation is based on its energy content rather than exergy. This is because market prices are generally tied to energy content. Using energy content for liquid biomethane aligns the economic assessment with market valuation practices and ensures consistency with fuel pricing.

The gross profit calculation varies by scenario which depends on the main product. For example, in Scenario 1, where the electricity is the main product, the selling price of the co-products (cooling and heating)

Table 1
Summary of process model results for Scenarios 1 and 2 across different CCS configurations (Arifianti et al., 2025).

Parameters	SCENARIO 1	l		SCENARIO 2	2		Unit
	Baseline	W/PRE-CCS	W/POST-CCS	Baseline	W/PRE-CCS	W/POST-CCS	
General operating conditions							
Air required in PG	10.10						kg/s
Steam required in PG	4						kg/s
Steam to CO ratio in WGSR	N/A	1.66	N/A	N/A	1.66	N/A	-
Cooling water	49.11	43.19	36.07	41.39	36.07	32.14	kg/s
CO ₂ captured	N/A	12.16	16.33	N/A	10.05	11.92	kg/s
Heat and power demand within the system							
Power for grinder and torch in PG	45.39						MW
Heat for AD	4.43						MW
Heat for stripper in CCS plant	N/A	40.29	58.18	N/A	34.30	42.90	MW
Power for compressors and pumps in CCS plant	N/A	4.40	7.60	N/A	3.70	5.80	MW
Power for compressors and pump in WS	N/A			1.49			MW
Power for compressor in ML	N/A			5.24			MW
Production							
Electricity	85.67	60.77	64.65	53.08	29.76	37.86	MW
Cooling energy	4.04	3.51	4.04	3.27	2.72	3.27	MW
Heating energy	17.29	27.87	26.84	13.99	25.62	17.12	MW
Liquid biomethane energy	N/A			43.26	43.26	43.26	MW
Process efficiency							
Overall energy efficiency	46.57	40.10	41.58	49.44	44.11	44.18	%
Overall exergy efficiency	35.55	25.92	27.70	41.20	32.22	35.70	%

Table 2 Parameters for conducting the DCFA.

Parameter	Description
Location	Indonesia
Plant life	20 years
Currency	USD
Base year	2023
Plant capacity	230 MW _{th} of feedstock
Discount rate	10 %
Tax rate	30 %
Construction period	3 years
First 12 months' expenditures	10 % of FCI
Next 12 months' expenditures	50 % of FCI
Last 12 months' expenditures	40 % of FCI
Depreciation method	Straight line
Depreciation period	10 years
Working capital	5 % of FCI
Electricity market price (Siahaan, 2025)	0.105 USD/kWh
Liquid natural gas (LNG) market price (Index Mundi, 2023)	0.049 USD/kWh
Vitrified slag price (Li et al., 2023)	53.78 USD/tonne
Indonesia's tipping fee (Erfinanto, 2024)	14.02 USD/tonne
Indonesia's carbon credit price (Revanda, 2025)	8.9 USD/tonne CO ₂

follows the electricity market price (refer to Table 2). In Scenario 2, where the liquid biomethane is the main product, the selling price of the co-products (electricity, cooling and heating) follows the electricity market price. The corresponding gross profit equations are presented in Equations (3) and (4).

where \dot{W}_{elec} is net electricity (in kWh), $\$_{cooling}$ and $\$_{heating}$ are equal to electricity market price ($\$_{elect}$) shown in Table 2, $\dot{E}x_{cooling}$ and $\dot{E}x_{heating}$ are the cooling and heating exergy (in kWh), respectively, COP_{cooler} was assumed to be 3.45 (Ratchawang et al., 2022), COP_{heater} was assumed to be 1. $\$_{slag}$ and \dot{m}_{slag} are the price of slag shown in Table 2 and mass flow rate of slag (in tonne/h), respectively. \dot{m}_{LBM} and LHV_{LBM} are the mass flow rate (in kg/s) and lower heating value of liquid biomethane (in kJ/kg), respectively. The tipping fee ($\$_{tipping}$) follows the Indonesian waste tipping fee of 14.02 USD/tonne (Erfinanto, 2024), with \dot{m}_{waste} representing the total waste processed. The carbon credit price ($\$_{carbon\ credit}$) is based on the Indonesian market at 8.9 USD/tonne CO₂ (Revanda, 2025). The capacity factor (C_f) and OPEX correspond to a process plant operating 8000 h per year.

In addition, to calculate the LCOWT, the main product and coproduct was assumed to be same as their market price, thus the gross profit equation for LCOWT calculation $(P_{n,wt})$ for Scenario 1 and 2 can be seen in Equations (5) and (6), respectively.

$$P_{n,Sc1} = \left(LCOE \times \dot{W}_{elec} + \$_{cooling} \times \frac{\dot{E}x_{cooling}}{COP_{cooler}} + \$_{heating} \times \frac{\dot{E}x_{heating}}{COP_{heater}} + \$_{slag} \times \dot{m}_{slag} + \$_{tipping} \times \dot{m}_{waste} + \$_{carbon\ credit} \times \dot{m}_{captured\ CO_2}\right) \times C_f \times 8000 - OPEX_n$$
 (Eq. 3)

$$P_{n.Sc2} = \left(LCObM \times \dot{m}_{LBM} \times LHV_{LBM} + \$_{elec} \times \dot{W}_{elec} + \$_{cooling} \times \frac{\dot{E}x_{cooling}}{COP_{cooler}} + \$_{heating} \times \frac{\dot{E}x_{heating}}{COP_{heater}} + \$_{slag} \times \dot{m}_{slag} + \$_{tipping} \times \dot{m}_{waste} + \$_{carbon\ credit} \times \dot{m}_{captured\ CO_2}\right) \times C_f \times 8000 - OPEX_n$$
(Eq. 4)

Table 3
The approach for estimating the CAPEX (Michailos et al., 2020), (Coppitters et al., 2021).

Expenses	Cost factor
A. Installed direct costs (IDC)	
(1) Total PEC	$1.00 \times PEC$
(2) Purchased equipment installation	$0.39 \times PEC$
(3) Instrumentation and controls	$0.26 \times PEC$
(4) Piping	$0.31 \times PEC$
(5) Electrical systems	$0.10 \times PEC$
B. Non-installed direct costs (NIDC)	
(1) Buildings	$0.55 \times PEC$
(2) Yard improvements	$0.12 \times PEC$
(3) Land	$0.06 \times PEC$
C. Total direct costs (TDC)	IDC + NIDC
D. Indirect costs (IC)	$0.255 \times PEC$
E. Fixed capital investment (FCI)	TDC + IC
F. Start-up costs	$0.05 \times FCI$
G. Interest during construction	Estimated
H. Total capital requirement (TCR)/CAPEX	$\mathbf{E} + \mathbf{F} + \mathbf{G}$
I. Working capital (WC)	$0.05 \times FCI$
J. Annualised CAPEX (ACAPEX)	$ ext{CAPEX} imes \left(rac{i_d imes (1+i_d)^n}{-1+\left(1+i_d ight)^n} ight)$

Table 5Chosen parameters for the sensitivity and uncertainty analysis.

Parameter	Low value	Nominal	High value	Unit
Economic assessr	nent			
PEC GT	70	100	150	%
PEC CCS	70	100	150	%
Carbon T&S	10.22	24.27	39.60	USD/tonne
Discount rate	8	10	12	%
Tax rate	0	30	40	%
Tipping fee	80	100	120	%
Carbon credit	80	100	120	%

approach, the cost of each component is represented as a fraction of the total purchased equipment cost (PEC), as detailed in Table 3. The capital cost contribution of each component is calculated by multiplying the total PEC by its corresponding factor. These factors are typically derived from historical cost data of comparable processes to ensure accuracy ('Capital Cost Estimating, 2013).

The estimation of PEC was carried out by utilizing the Aspen Plus economic evaluation software in conjunction with the baseline cost equation derived from prior research studies. Aspen Plus was used to

$$P_{n,wt,sc1} = \left(LCOWT \times \dot{m}_{waste} + \$_{elec} \times \dot{W}_{elec} + \$_{cooling} \times \frac{\dot{E}x_{cooling}}{COP_{cooler}} + \$_{heating} \times \frac{\dot{E}x_{heating}}{COP_{heater}} + \$_{slag} \times \dot{m}_{slag} + \$_{tipping} \times \dot{m}_{waste} + \$_{carbon\ credit} \times \dot{m}_{captured\ CO_2}\right) \times C_f \times 8000$$

$$- OPEX_n$$
(Eq. 5)

$$P_{n,wt,sc2} = \left(LCOWT \times \dot{m}_{waste} + \$_{LNG} \times \dot{m}_{LBM} \times LHV_{LBM} + \$_{elec} \times \dot{W}_{elec} + \$_{cooling} \times \frac{\dot{E}x_{cooling}}{COP_{cooler}} + \$_{heating} \times \frac{\dot{E}x_{heating}}{COP_{heater}} + \$_{slag} \times \dot{m}_{slag} + \$_{tipping} \times \dot{m}_{waste} + \$_{carbon\ credit} \times \dot{m}_{captured\ CO_2}\right) \times C_f \times 8000 - OPEX_n$$
(Eq. 6)

Where $\$_{LNG}$ is the liquid natural gas market price, as shown in Table 2. To calculate the LCOWT, LCOE, and LCObM, two key metrics,

To calculate the LCOWT, LCOE, and LCObM, two key metrics, namely capital expenditure (CAPEX) and operating expenditure (OPEX), need to be determined. The calculation of CAPEX involves the utilization of a methodology referred to as the bottom-up approach. In this

calculate PEC for standard process items (e.g., condensers, evaporators, and pumps; see Table S3 in the **Supplementary Information** for detailed values). Nevertheless, for equipment involving complex simulation models, such as PG, AD, WGSR, and the CCS plant, the Aspen Plus database has certain limitations. To address this, baseline price

Table 4PEC at base capacity, PEC formulation and year of reference.

Equipment	Base cost [MM USD]	Base capacity	Unit	Scaling factor	Base year	Ref.	CEPCI
Crusher	2	2000	ton/day (dry feed mass flow)	0.72	2007	Dimitriou et al. (2018)	525.4
Drier	19.3	2000	ton/day (dry feed mass flow)	0.72	2007	Dimitriou et al. (2018)	525.4
Plasma gasifier	78	39.2	kg/s (feed mass flow)	0.67	2021	Chen et al. (2022)	708.8
Substrate heater	0.693	13,149	m ² (heat transfer area)	0.68	2014	Han and Sun (2020)	576.1
Anaerobic digester	0.455	727.21	m ³ (feed volume flow)	1	2017	Lin et al. (2019)	567.5
Desorber	0.0175	100	m ² (heat transfer area)	0.6	2000	Alelyani et al. (2017)	394.1
Absorber	0.0165	100	m ² (heat transfer area)	0.6	2000	Alelyani et al. (2017)	394.1
Solution heat exchanger	0.012	100	m ² (heat transfer area)	0.6	2000	Alelyani et al. (2017)	394.1
WGSR	3.77	150	kg/s (total gas feed)	0.67	2014	Albrecht et al. (2017)	576.1
Burner ^a	2.14	20	MW (heat duty)	0.83	2014	Albrecht et al. (2017)	576.1
Cooling tower	3.99	4530.3	kg/s (feed mass flow)	0.78	2014	Onel et al. (2015)	576.1
Heat exchanger	0.8	8372	m ² (heat transfer area)	0.68	2014	Han and Sun (2020)	576.1
Air compressor (AC)	$PEC_{AC} = \frac{71.1 \dot{m}_{AC}}{0.9 - \eta_{AC}} \left(\frac{P_{AC}}{P_{AC}}\right)$	$\frac{AC,out}{AC,in}$ $ln\left(\frac{P_{AC,out}}{P_{AC,in}}\right)$		0.7 ^b	1994	Wang et al. (2021)	368.1
	Here, \dot{m}_{AC} denotes the	mass flow rate th	rough the AC, η_{AC} represents its				
	isentropic efficiency, a	nd $P_{AC,in}$ and $P_{AC,in}$	out are the fluid pressures at the air				
	compressor's inlet and	outlet, respective	ely.				
CCS plant	The PEC of all compon	ents (compressor	s, pumps, heat exchangers, columns)	0.7 ^c	2022	Mullen and Lucquiaud (2024)	816
	in the CCS plant is esti	mated using the f	inancial calculations provided in the				
	referenced study						

^a The burner combusts a 10 % of raw syngas and generates heat to supply steam required for the WGSR process.

^b The scale factor value (0.7) is taken from Reference (Albrecht et al., 2017).

^c The scale factor value (0.7) is taken from Reference (Yang et al., 2021).

equations from previous studies were used, as shown in Table 4. To account for the changes in the equipment capacity and the year of the economic analysis between the current study and the referenced one, Equation (7) was used.

$$C = C_0 \left(\frac{S}{S_0}\right)^f \times \left(\frac{I_{current}}{I_0}\right)$$
 (Eq. 7)

where C represents the cost of the unit while it is operating at its actual capacity (S). C_0 denotes the base cost of the unit at a given base size or capacity (S_0) . The scaling capacity factor, denoted as f, varies depending on the type of process equipment. $I_{current}$ and I_0 are the indexes taken from the Chemical Engineering Plant Cost Index (CEPCI) for the year of the current study and the year of the referenced base cost from the literature, respectively.

Alongside CAPEX, OPEX comprises any ongoing costs related to normal operations of a plant. OPEX is defined by the sum of the fixed operating and maintenance costs (FOM) and variable operating costs (VC). The detailed methodology and assumptions used to calculate OPEX are provided in the **Supplementary Information** (Section S.2).

2.4. Sensitivity and uncertainty analysis for the economic investigation

Sensitivity and uncertainty analyses are conducted to ensure consistency and reliability of the economic evaluation which assists in identifying the most influential input parameters affecting the estimated indicators. A local sensitivity analysis is performed by varying one parameter at a time while keeping all other parameters constant. Table 5 provides a summary of the independent variables along with their respective lower and upper bounds. These parameters were chosen due to their significant levels of uncertainty. The low and high ranges for PEC were derived from the classification guidelines of AACE International, which apply to plants with low maturity levels, such as WtE process plants (Bates et al., 2005). Specifically, the PEC values were assumed to vary between $-30\ \%$ and $+50\ \%$.

The low, median, and high estimates for CO_2 transportation and storage costs are based on the 2016 UK Department of Energy and Climate Change report (DECC, 2016), since Indonesia has not yet implemented CCS technology, with its first CCS project targeted for operation in 2030 (Limanseto, 2025). Other parameters are aligned with typical market-relevant factors, such as tax rates and discount rates (Michailos et al., 2020). The tax rate ranges from a minimum of 0 %, accounting for potential tax exemptions, to a maximum of 40 %. The discount rate reflects project investment risk, with a lower bound of 8 % and an upper bound of 12 %. Tipping fee and carbon credit prices are based on Indonesian median values, with ± 20 % variation applied following previous studies on investment incentives for plasma gasification combined cycle power plants utilizing municipal solid waste (MSW) (Montiel-Bohórquez et al., 2022).

To assess the combined impact of variations in uncertain parameters on the LCOE, LCObM, and LCOWT, a well-known statistical method, such as Monte Carlo simulation, is employed. The input parameters and their respective value ranges, which reflect plausible variability based on literature and current market conditions, are detailed in Table 5. Using Matlab, 10,000 simulation trials were performed, each randomly sampling values within these specified ranges according to predefined distributions.

This extensive sampling allowed for the generation of probability distribution curves for LCOE, LCObM, and LCOWT, from which 95 % confidence intervals (CI) were determined. These CI provide a robust measure of uncertainty around the mean cost estimates. Furthermore, key statistical metrics, including the mean, median, and standard deviation (STD), were computed from the simulation results to summarize the central tendency and variability of the cost outcomes.

2.5. Environmental evaluation

The environmental impacts of the proposed waste treatment scenarios are quantified using a cradle-to-gate approach, in accordance with International Organization for Standardization (ISO) 14040 standards. The assessment excludes the distribution, usage, and final disposal stages. The LCA was conducted using the SimaPro V.9 software and followed a standardized four-step process: goal and scope definition, inventory analysis, impact assessment, and interpretation. The analysis was based on the system boundaries defined in Figs. 1 and 2, focusing on input and output flows while excluding the detailed modelling of internal processes.

2.5.1. Goal and scope definition, functional unit

The goal of this LCA study is to evaluate and compare the environmental sustainability of converting municipal waste (plastic and food waste) into CCHP production in Scenario 1 and CCHP combined with liquid biomethane production in Scenario 2, including their three respective cases. In an LCA study, selecting the functional unit (FU) is critical, as it significantly influences the outcomes and must align with the study's goal and scope. For this study, the chosen FUs are 1 kg of waste, comprising 74 % food waste and 26 % plastic waste. The analysis assumes a plant lifespan of 20 years.

2.5.2. Life cycle inventory (LCI)

Two primary sources were utilized to construct the LCI for this study. The first source comprises mass and energy balances derived from process modelling conducted in Aspen Plus. This dataset includes standardized values for converting primary raw materials into CCHP and liquid biomethane, measured per kilogram of plastic and food waste. It also encompasses data on a wide range of pollutants and waste streams generated during the conversion process.

The second data source is the "Ecoinvent-3" database, which provides comprehensive inventories accessible through the SimaPro tool. The system model "allocation, cut-off by classification system" method is used. The implementation of Scenarios 1 and 2 is planned for Indonesia; therefore, Indonesia-specific LCI data is prioritized. However, if such data is unavailable, the "Rest of the World" databases were used as alternatives.

For the current assessment, the inventory for infrastructure construction relies on existing data from the Ecoinvent database. The estimation of inventory requirements for newly constructed infrastructure is determined using the six-tenths factor rule, as represented in the following equation (Cuéllar-Franca et al., 2019), (Fernanda Rojas Michaga et al., 2022).

$$IP_2 = IP_1 \left(\frac{CPP_2}{CPP_1}\right)^k$$
 (Eq. 8)

In this equation, IP_1 represents the capacity proportion of the original Ecoinvent process plant, while IP_2 denotes the capacity proportion required for the equivalent process in the observed system. CPP_1 and CPP_2 refer to the capacities of the original Ecoinvent process plant and the observed system. The parameter k is the scaling factor, typically set to 0.6 (Cuéllar-Franca et al., 2019), which accounts for the non-linear relationship between capacity and proportional requirements.

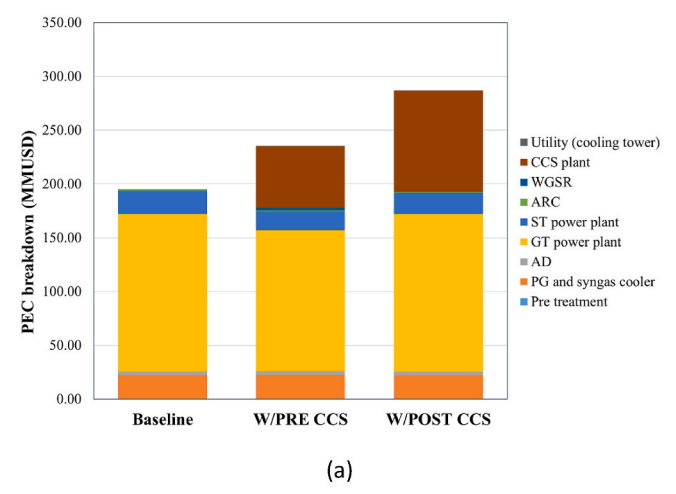
2.5.3. Life cycle impact assessment (LCIA)

In this study, the LCIA was conducted using the ReCiPe 2016 midpoint (H) method. The midpoint approach provides a detailed understanding of emissions distribution across various stages of energy production by calculating 18 midpoint impact categories. Since the system involves two distinct types of carbon waste, fossil origin waste (plastic waste) and biogenic origin waste (food waste), it is necessary to differentiate between these sources when calculating carbon emissions. This is achieved by determining the ratio of biogenic carbon in biogas

from food waste to fossil carbon in syngas from plastic waste. This ratio helps identify the contributions of biogenic carbon and fossil carbon to overall emissions. Thus, in the inventory under the "Emissions to air" category, carbon emissions are classified as "Carbon dioxide, fossil" "Carbon dioxide, biogenic" "Carbon monoxide, fossil" and "Carbon monoxide, biogenic."

For cases involving CCS plants, captured biogenic CO_2 is considered as "negative emission," with a characterization factor of minus one under "Carbon dioxide" in the "Emissions to air" category. However, in the observed system, the captured CO_2 is not entirely biogenic. In Scenario 1, there is a mixture of captured biogenic and fossil CO_2 , while Scenario 2 involves fully captured fossil CO_2 . For the mixed case in Scenario 1, the previously determined ratio is used to calculate the amount of captured biogenic carbon. For example, if the captured biogenic carbon ratio is 0.27, the characterization factor becomes minus 0.27. Conversely, for cases with fully captured fossil CO_2 , the characterization factor is set to zero.

When the investigated system generates a variety of products, the allocation technique must be implemented to distribute LCI data and environmental impact (Chen et al., 2019), (Ekvall and Finnveden, 2001). The allocation approach involves the assignment of emissions to products in accordance with their flow characteristics, which may include the mass, energy, or carbon content, or the economic value of those products (Von Der Assen et al., 2013). While all the products in both scenarios are associated with some type of energy, the quality of energy varies, resulting in unequal work potential for various outputs (Jana and De, 2016). Thus, this study employs an allocation method



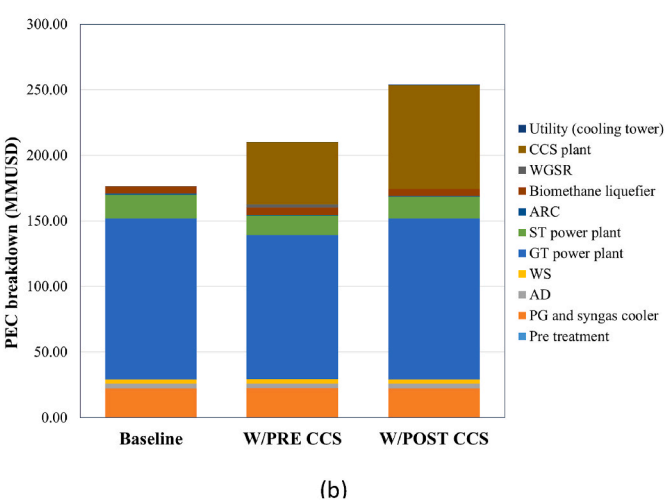


Fig. 3. Contribution of each component to the total PEC for (a) Scenario 1 and (b) Scenario 2.

Table 6
CAPEX and annualised CAPEX (ACAPEX) for scenario 1 and scenario 2.

Parameters	Scenario 1	_		Scenario 2	2	
	Baseline	W/pre- CCS	W/ post- CCS	Baseline	W/pre- CCS	W/ post- CCS
CAPEX (MMUSD)	635.52	767.00	935.32	575.67	685.76	827.40
ACAPEX (MMUSD)	74.65	90.09	109.86	67.62	80.55	97.19

based on the exergy value of the product. Similar allocation can be found in prior studies, such as (Díaz-Ramírez et al., 2023), (Bhering Trindade et al., 2021), (Choi et al., 2022).

2.6. Limitation of the study

It is important to acknowledge that the uncertainty analysis in this study was focused on the economic evaluation, specifically on the LCOE, LCObM, and LCOWT. This focus reflects the practical and immediate importance of economic variability for decision-making in WtE projects. Uncertainties related to the Aspen Plus process model, including feed-stock composition, operating conditions, and reaction kinetics, require detailed data and extensive computational resources to analyze thoroughly. Such process-level uncertainty analyses are complex and often conducted in subsequent research stages.

By addressing economic uncertainties initially, this study provides valuable insights into the financial robustness of the proposed system. Future work will integrate process model uncertainties alongside economic uncertainties to offer a more comprehensive evaluation of system performance and sustainability.

3. Result and discussion

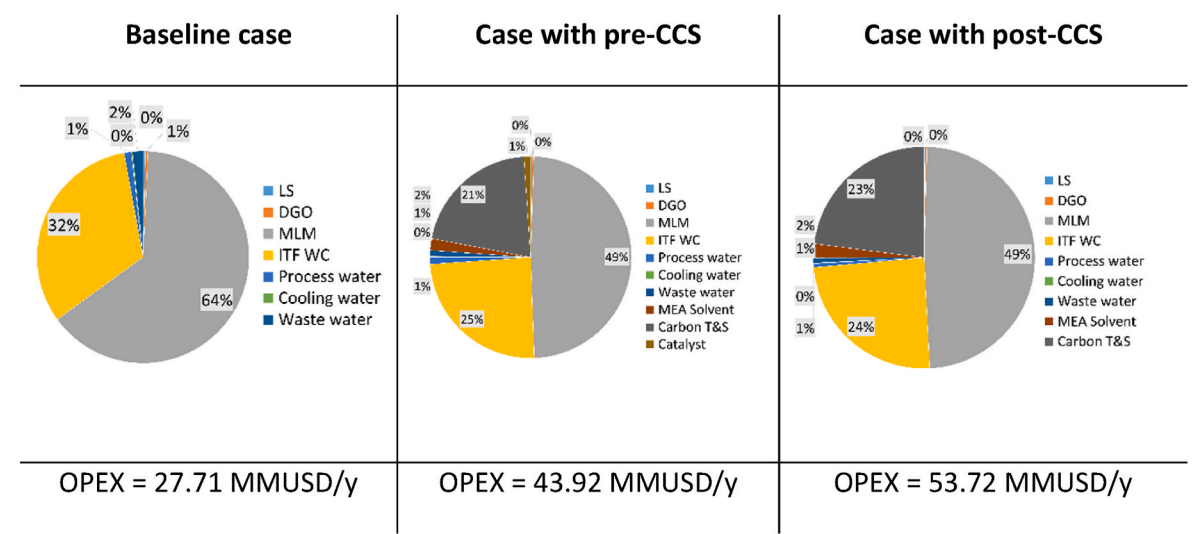
3.1. Economic performance

3.1.1. LCOE, LCObM, and LCOWT

Fig. 3a and b illustrate the PEC breakdown for Scenarios 1 and 2, respectively. The total PEC for Scenario 1 ranges from 194 to 287 MMUSD, while for Scenario 2, it ranges from 176 to 254 MMUSD depending on the adopted case. From the figures, the GT power plant represents the most significant cost component across all cases, primarily due to the high price of the gas turbine. This is followed by the PG in the baseline cases of both scenarios. These findings align with previous studies by Aich et al. (2024) and Tang et al. (2023), which reported that the investment cost of a PG is lower than that of the power generation unit.

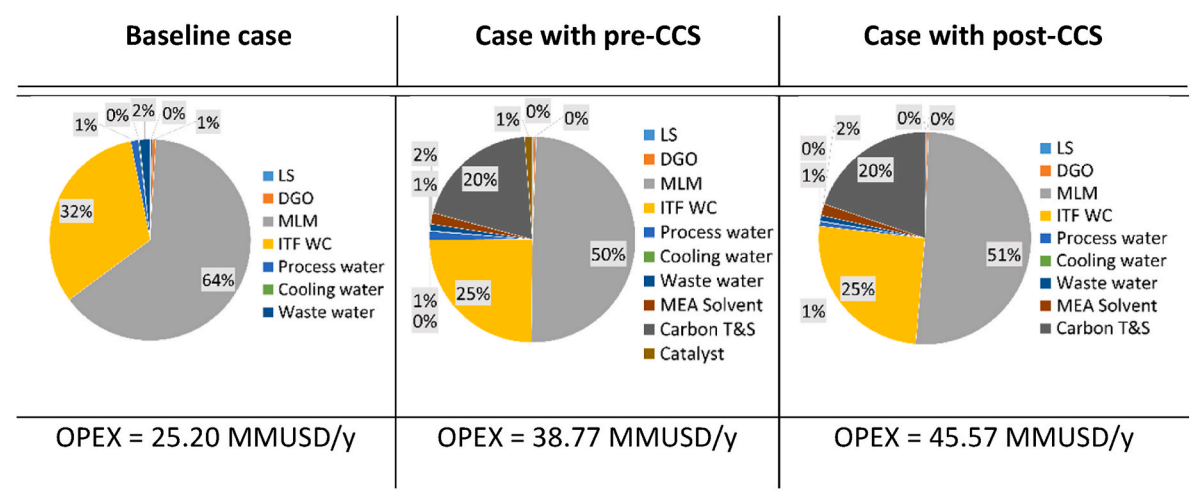
Meanwhile, in the cases involving CCS plants, the CCS plant emerges as the second most significant cost component after the GT power plant. This observation is consistent with prior studies on the integrated gasification combined cycles with CO₂ capture (Ghiat et al., 2020), (Zang et al., 2018). Furthermore, the cost of the CCS plant in the pre-CCS case is lower than in the post-CCS case, due to the smaller amount of feed gas processed. The PEC directly influences CAPEX, which is calculated based on the methodology outlined in Table 3. As observed in Table 6, Scenario 1 incurs a higher CAPEX than Scenario 2. Across all cases, the baseline configuration has the lowest CAPEX, followed by the pre-CCS case, while the post-CCS case exhibits the highest CAPEX.

Fig. 4a and b present the OPEX breakdown for Scenarios 1 and 2, respectively, along with their estimated total OPEX. For Scenario 1, the total OPEX ranges from 27 to 54 MMUSD/year, whereas for Scenario 2, it ranges from 25 to 46 MMUSD/year depending on the adopted case. In both scenarios, the post-CCS case has the highest OPEX, while the baseline case has the lowest. The higher OPEX in CCS cases compared to the baseline case is primarily due to significant variable costs associated



Note: LS (Labour and supervision), DGO (Direct and general overhead), MLM (Maintenance labour and materials), ITF WC (Insurance, tax and financing WC)

(a)



Note: LS (Labour and supervision), DGO (Direct and general overhead), MLM (Maintenance labour and materials), ITF WC (Insurance, tax and financing WC)

(b)

 $\textbf{Fig. 4.} \ \ \textbf{OPEX} \ \ \textbf{breakdown for (a) Scenario 1 and (b) Scenario 2}.$

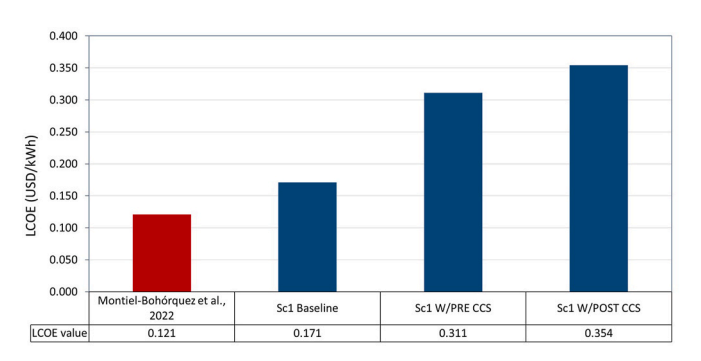


Fig. 5. LCOE comparison for Scenario 1: baseline, pre-CCS, and post-CCS cases, with the literature value (Montiel-Bohórquez et al., 2022).

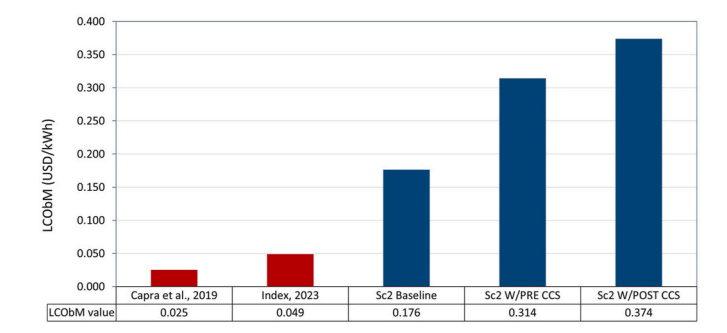


Fig. 6. LCObM comparison for Scenario 2: baseline, pre-CCS, and post-CCS cases, with the literature value (Index Mundi, 2023), (Capra et al., 2019).

with carbon transport and storage (carbon T&S).

In terms of the OPEX distribution, "maintenance labour and materials" account for the largest percentage in both scenarios. In the baseline cases, the second-largest component is "insurance, tax, and financing WC", while in the CCS cases, the second-largest cost is attributed to Carbon T&S. It is worth mentioning that OPEX excludes both feedstock costs, which are free, and feedstock transportation costs since the proposed system is located at the landfill site. Comparing the ACAPEX values from Table 6 with the OPEX indicates that annual CAPEX exceeds OPEX, which signifies that the financial structure of the current system is more CAPEX-driven.

Fig. 5 presents a comparison of the LCOE in Scenario 1 with values reported in the literature (Montiel-Bohórquez et al., 2022). The reference study describes an integrated plasma gasification combined cycle power plant comprising a PG, fabric filter, wet scrubber, COS-hydrolysis unit, $\rm H_2S$ removal, sour water treatment systems, and a CCGT. The LCOE values used for comparison are from the baseline case in the reference study, where no incentives, such as waste treatment fees, are applied. This approach ensures a consistent basis for evaluation.

Despite the absence of incentives, the LCOE reported in the literature remains significantly lower than those in all cases of Scenario 1, particularly in configurations involving CCS. The specific capital cost in the reference study is approximately 298,543 USD per tonne of MSW processed per day (Montiel-Bohórquez et al., 2022), whereas in the current study it ranges from 387,705 to 570,625 USD per tonne of MSW. This substantial difference can be attributed to several factors. Firstly, the size of the CCGT differs: the reference case reports a gross electricity output of 99.1 MW, while the current study's baseline, pre-CCS, and post-CCS cases produce 131.06 MW, 110.54 MW, and 117.64 MW, respectively. Fig. 3a indicates that the CCGT is the largest contributor to PEC, thus its size significantly influences the specific capital cost.

Secondly, the reference study employs a simpler process configuration, excluding components such as the ARC, AD, and WGSR. Additionally, the smaller feedstock throughput in the reference case (900 tonnes MSW/day versus 1639 tonnes MSW/day in this study) likely results in a smaller CCS plant and consequently lower PEC for CCS. As illustrated in Fig. 3a, the CCS plant represents the second-largest PEC contributor after the CCGT.

Fig. 6 presents the LCObM results for Scenario 2, comparing the current study's outcomes with the reference case from Capra et al., (2019) and the LNG price in Indonesia (Index Mundi, 2023). The LCObM values for all cases in Scenario 2 are more than four times higher than both reference benchmarks. This difference is primarily because Capra et al., (2019) focus solely on converting biogas into liquid biomethane using a simpler process that includes AD, raw biogas pre-treatment, upgrading and polishing units, and liquefaction. In contrast, the current study integrates multiple complex technologies, such as PG, AD, CCGT, ARC, WS, ML, and CCS resulting in significantly higher CAPEX.

The CAPEX is heavily influenced by the PEC. As shown in Fig. 3b, the

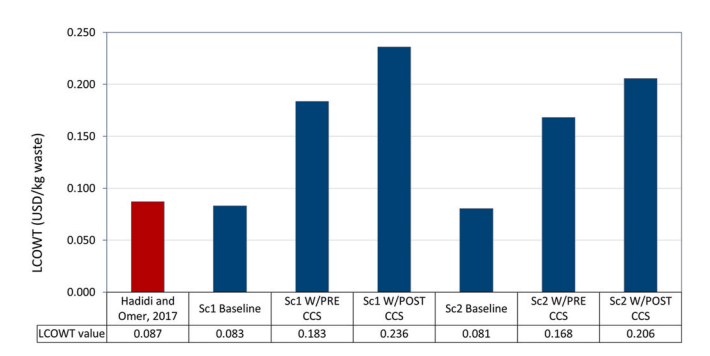


Fig. 7. Comparison of the LCOWT for Scenarios 1 and 2 under different configurations: baseline, pre-CCS, and post-CCS, along with the literature value from (Hadidi and Omer, 2017).

Table 7Comparison of the current multi-output generation system's performance against single-output generation systems reported in the literature.

Feedstock	Plant Capacity	Economic performance	Main component within the system	Reference
Mixed 5 kg/s of plastic & 13.97 kg/s of food	60.77–85.67 MW of electricity, cooling, and heating biomethane	CAPEX: 635.52–935.32 MMUSD LCOE: 0.172–0.3542 USD/kWh	PG, AD, CCGT, ARC, and CCS	Current study
waste (total waste = 2222.62 tonnes/day)	Electricity, cooling, heating, and 43.26 MW of biomethane	CAPEX: 575.67–827.40 MMUSD LCObM: 0.1762–0.3737 USD/kWh	PG, AD, CCGT, ARC, WS, ML, and CCS	Current study
200 tonnes/ day of OFMSW	30.41 Nm ³ Biomethane/ MT OFMSW	CAPEX: ~44.9 MM USD Biomethane price: 0.554 USD/Nm ³	AD and absorption column	Anaya-Reza et al. (2022)
	126,400 kWh of electricity/ day	CAPEX: ~49.5 MMUSD Standard electricity price: 0.071 USD/kWh	AD, H ₂ S removal, steam generator, and steam turbine	Anaya-Reza et al. (2022)
30 tonnes of corn stover, 149 tonnes of	744 GJ of biomethane	CAPEX: 522,799 USD Biomethane price: 0.54 USD/m ³	AD and HPWS	Li et al. (2020)
tomato residues, 250 tonnes of dairy manure	61,995 kWh of electricity, and 314.1 GJ of heat	CAPEX: 602,981 USD Electricity selling price: 0.16 USD/kWh Heat energy selling price: 0.04 USD/kWh	AD and CHP engines	Li et al. (2020)
50 tonnes/ day of plastic waste	1850 kWh of electricity/ton of plastic waste	Equipment cost: 1.5 MMUSD Electricity selling price: 0.142 USD/kWh	Gasifier, WGSR, gas purifier, CHP system	Javed et al. (2025)
0.95 tonnes/h of end- belt refuse	4 MWe	Total plant cost: 4.79 k€/kWe	Fluidized bed gasifier, cyclone, syngas combustor, heat recovery steam generator, steam turbine	Arena et al. (2011)

largest PEC contribution comes from the CCGT, with costs of 140.91, 124.65, and 139.14 MMUSD for the baseline, pre-CCS, and post-CCS cases, respectively. This is followed by the CCS plant, with PECs of 47.48 and 79.11 MMUSD for the pre-CCS and post-CCS cases, respectively. The PG also represents a substantial cost, with a PEC around 22 MMUSD. These significant equipment costs contribute to the higher LCObM observed in the current study.

Furthermore, the LCObM reported in this study exceeds the current Indonesian LNG market price (Index Mundi, 2023) for domestic LNG production plants. This discrepancy arises from the comparatively smaller scale of the system analyzed in this study. Since LNG plants are typically large-scale facilities, they benefit from economies of scale which significantly reduces their production costs.

The LCOWT is calculated by assuming the main product, coproducts, and by-products sold using market price, as detailed in Equations (5) and (6). Fig. 7 compares LCOWT values across both scenarios with those from the literature (Hadidi and Omer, 2017), where the reference system utilized a bubble fluidized bed gasifier, syngas cleaner, and combustion engines. LCOWT values in all baseline cases are comparable to the reference. However, CCS cases show LCOWT values approximately double those of the baseline and reference cases, primarily due to the additional costs of integrating a CCS plant.

The LCOWT in Scenario 1 is slightly higher than in Scenario 2, and this is primarily due to the significantly higher CAPEX in Scenario 1. The higher CAPEX observed in Scenario 1 is primarily attributed to the CCGT system's increased size and associated equipment costs. Scenario 1 employs a CCGT fueled by a mixture of syngas from plastic waste plasma gasification and biogas from food waste anaerobic digestion, necessitating a larger gas turbine to handle the greater fuel volume. Conversely, Scenario 2's gas turbine is fueled solely by syngas from plasma gasification, as biogas is converted into liquid biomethane separately, allowing for a smaller, less expensive CCGT system. This difference in fuel strategy directly impacts the size and cost of the CCGT, leading to the higher CAPEX in Scenario 1.

Additionally, Scenario 1 incurs to be slightly higher OPEX compared to Scenario 2. Revenue differences also contribute to the LCOWT variation between the two scenarios. In Scenario 1, the primary product is electricity, with an annual production ranging between 486 GWh and 686 GWh. In contrast, Scenario 2 primarily produces liquid biomethane, with an annual output of 346 GWh. Since the market price of electricity is approximately twice that of liquid biomethane, this pricing disparity further influences the difference in LCOWT between the two scenarios.

3.1.2. Comparison with single-output WtE systems

To contextualize the techno-economic performance of the proposed multi-output WtE system, a comparison with single-output systems

documented in the literature is presented in Table 7. The present study investigates two scenarios processing mixed plastic and food waste, producing multiple outputs including CCHP, and biomethane, with CAPEX ranging from approximately 576 to 935 MMUSD, LCOE between 0.172 and 0.354 USD/kWh, and LCObM between 0.176 and 0.374 USD/kWh

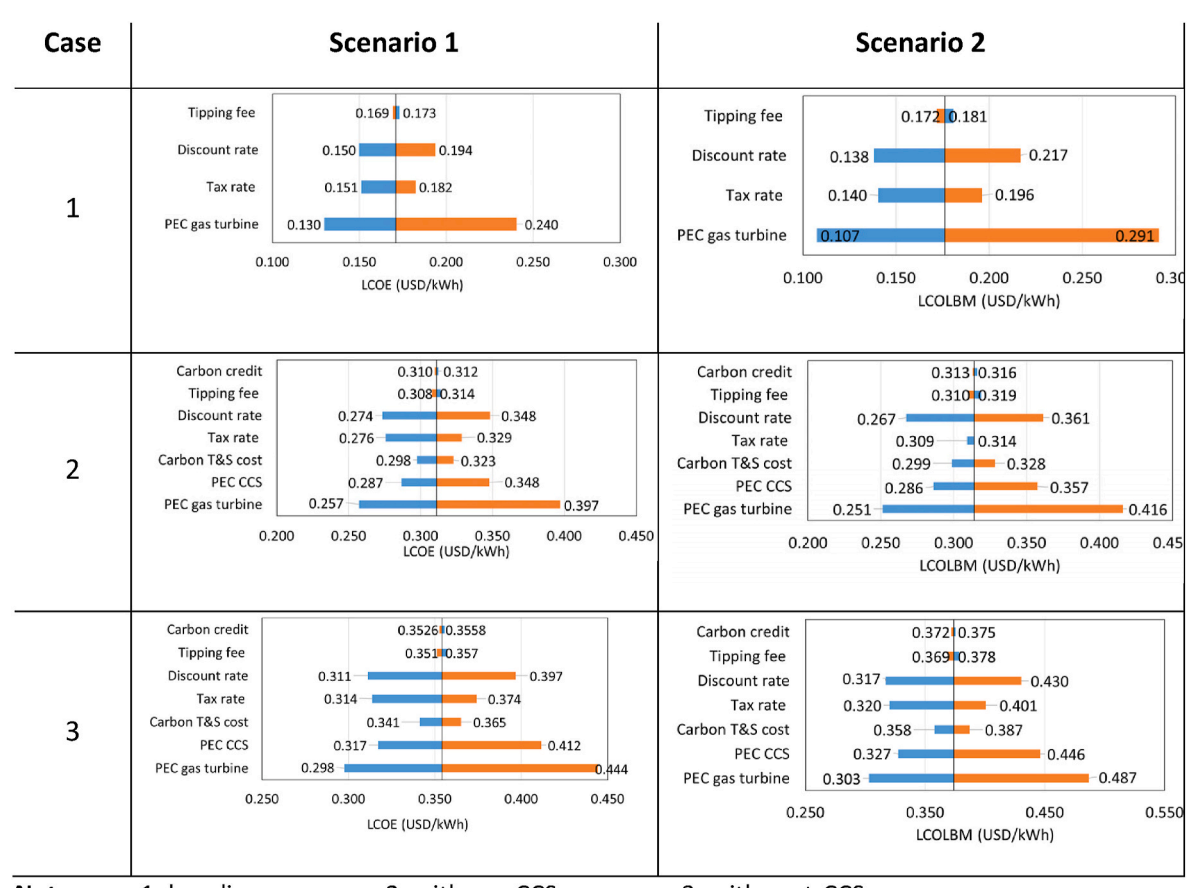
Anaya-Reza et al. (2022) report lower CAPEX per tonne of waste for their baseline biomethane production system compared to the baseline biomethane scenario in this study, supporting that multi-output configurations typically incur higher capital costs relative to single-output systems. Their work further highlights that combined heat and power (CHP) systems, as non-single-output configurations, exhibit increased CAPEX, a trend also observed by Li et al. (2020), where biomethane-only systems present lower CAPEX than CHP systems.

Similarly, single-output electricity generation from plastic waste, as investigated by Javed et al. (2025) and Arena et al. (2011), demonstrates lower CAPEX than the integrated multi-output system examined herein. This comparative analysis underscores that the greater process complexity in multi-output systems contributes to elevated capital requirements, reflecting the trade-off between enhanced functionality and increased investment. Further, multi-output systems have the potential to diversify revenue streams and enhance system adaptability.

3.1.3. LCOE, LCObM, and LCOWT sensitivity analysis

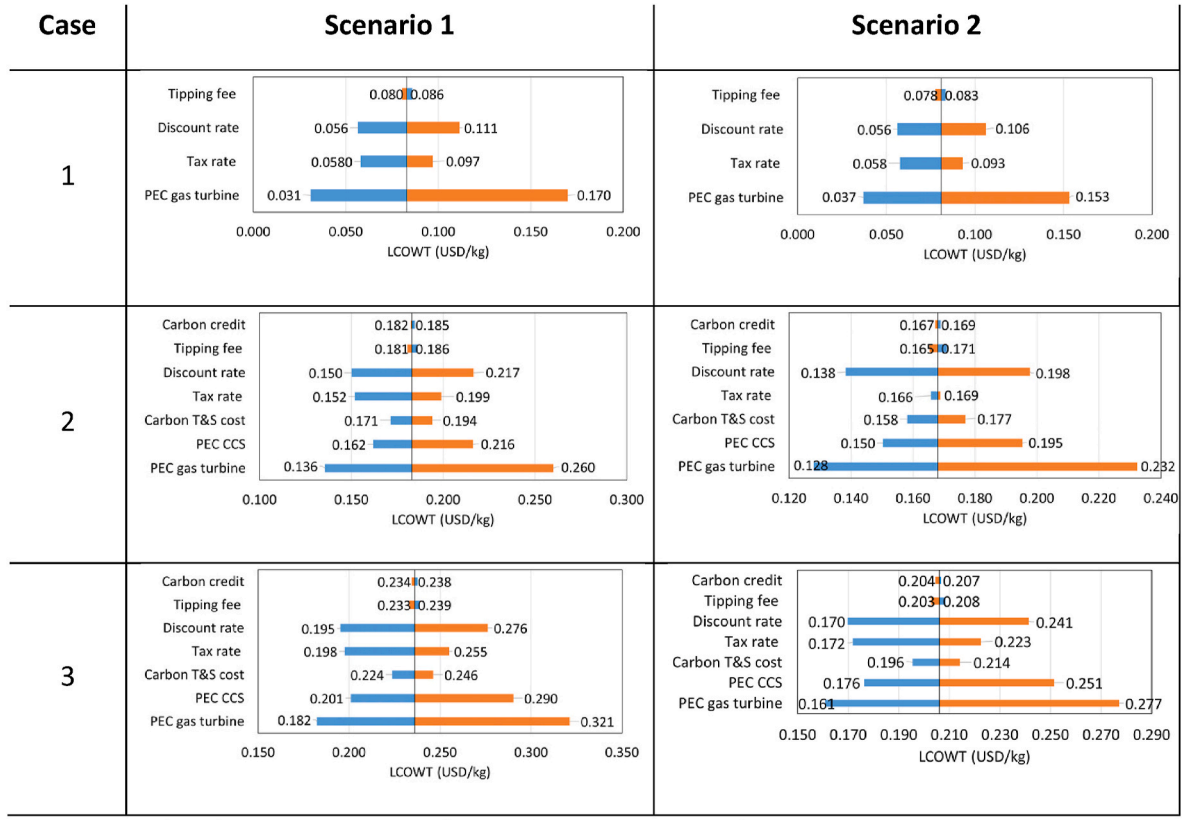
Fig. 8 presents the results of the sensitivity analysis on the LCOE and LCObM, while Fig. 9 illustrates the sensitivity analysis on the LCOWT. In all cases, the PEC of the GT emerges as the next most influential parameter. This significant impact is attributed to the fact that the GT is the most expensive component in each case across both scenarios.

Since most plastics are derived from fossil fuels, capturing fossilbased carbon emissions during the utilization of syngas from the



Note: case 1: baseline case; case 2: with pre-CCS case; case 3: with post-CCS case

Fig. 8. Sensitivity of the LCOE and LCObM to various economic variables.



Note: case 1: baseline case; case 2: with pre-CCS case; case 3: with post-CCS case

Fig. 9. Sensitivity of the LCOWT to various economic variables.

Table 8The output of the system under different proportion.

Output (MW)	Baseline			W/PRE-CCS			W/POST-CCS			
	24:76	50:50	90:10	24:76	50:50	90:10	24:76	50:50	90:10	
Scenario 1										
Electricity	85.67	133.79	213.94	60.77	93.76	150.1	64.65	100.47	162.17	
Cooling	0.34	0.56	0.95	0.29	0.48	0.81	0.34	0.56	0.95	
Heating	1.62	2.69	4.51	2.83	4.65	7.82	3.28	2.72	9.11	
Scenario 2										
Electricity	53.08	111.7	209.55	29.76	73.9	145.72	37.86	81.54	154.33	
Cooling	0.27	0.52	0.94	0.23	0.44	0.8	0.27	0.52	0.94	
Heating	1.49	2.61	4.5	2.7	4.57	7.81	3.13	2.61	9.06	
Liquid methane	43.26	29.26	5.81	43.26	29.26	5.81	43.26	29.26	5.81	

plasma gasification of plastic waste is essential. To achieve net-zero emissions, biogenic carbon from the biogas also needs to be captured. Consequently, the costs of implementing CCS technology have a significant impact on the LCOE, LCObM, and LCOWT. As shown in Figs. 8 and 9, the PEC of CCS gives impact on the LCOE, LCObM and LCOWT. The future cost of CCS equipment could decrease due to technological advancements and economies of scale, as highlighted in (Lan and Yao, 2022). Both Figs. 8 and 9 also demonstrate that the effect of carbon T&S costs is relatively small. The adoption of T&S facilities depends more on the social factors and public acceptance rather than economic considerations (Michailos et al., 2019).

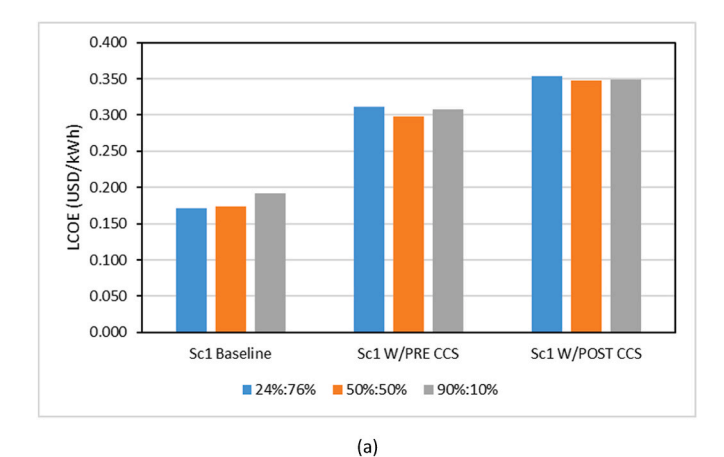
Among common financial factors, the discount rate shows a broader fluctuation range compared to the tax rate. Small changes in the discount rate can lead to substantial variations in the LCOE, LCObM, and LCOWT. While tax allowances can improve the project viability, their impact is limited since even under an optimistic tax-free scenario, the LCOE, LCObM, and LCOWT would only decrease by less than 17 %. Policy-driven incentives, namely the waste tipping fee and carbon credit

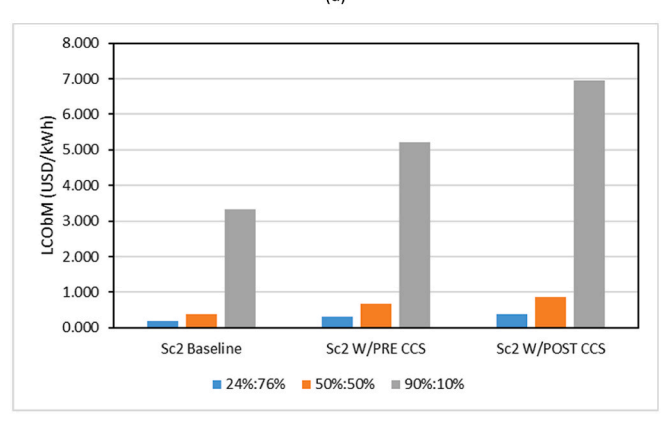
price, have only a minimal effect on project unit costs.

3.1.4. Feedstock composition sensitivity analysis

In municipal refuse, the proportion of plastics and food waste can vary widely; to quantify its impact on system economics, three PW:FW blends (24:76, 50:50 and 90:10) were simulated in Aspen Plus. For each case, all unit operations were resized and mass-/energy-balance outputs compiled (Table 8), then subjected to DCFA to yield the LCOE in Scenario 1, the LCObM in Scenario 2, and the LCOWT in both scenarios.

As shown in Table 8, increasing the plastic-to-food waste ratio from 24:76 to 90:10 results in a marked shift in the main outputs. Electricity production in both Scenario 1 and Scenario 2 rises with higher plastic content, owing to the greater calorific density of plastics, which yields a more energetic fuel gas stream. Conversely, liquid biomethane output in Scenario 2 declines substantially as the proportion of biodegradable food waste is reduced, diminishing the biogas volume available for upgrading. As a result, the gap between electricity and biomethane outputs widens with more plastic content, highlighting how feedstock





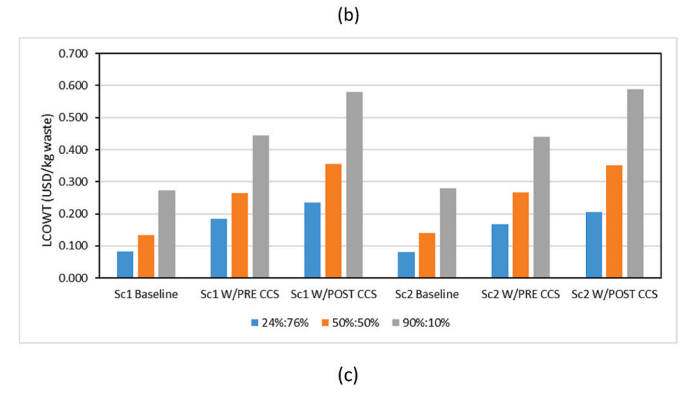


Fig. 10. Sensitivity of levelized costs to feedstock composition. (a) LCOE in Scenario 1 (CCHP), (b) LCObM in Scenario 2 (CCHP + biomethane), and (c) LCOWT as the plastic-to-food waste ratio varies (24:76, 50:50, 90:10) under baseline, pre CCS, and post CCS configurations.

composition determines whether the system favours power generation or biomethane production.

Fig. 10a–c presents the corresponding levelized costs. Total CAPEX rises with plastic content due to a larger plasma gasifier plus upsized CCGT and CCS units; nevertheless, LCOE in Scenario 1 remains relatively insensitive. This stability occurs because the higher plastic content produces a more energy-dense syngas stream, boosting electricity output and offsetting the added capital costs. In Scenario 2, by contrast, LCObM climbs sharply between the 50:50 and 90:10 blends. Although CAPEX for biomethane-specific equipment (AD, WS, and liquefaction) falls with reduced biogas flow, the higher CAPEX for processing the plastic-rich feed must still be recovered over a shrinking methane volume. Note that electricity revenue in Scenario 2 is assumed at prevailing market prices rather than the levelized cost derived from DCFA, as in Scenario 1.

Fig. 10c shows how LCOWT varies with feedstock composition. Here, LCOWT is calculated by assuming that all outputs (CCHP, and biomethane) are sold at market prices. As the plastic fraction increases, LCOWT rises because plastic-rich feeds require more capital and energy for gasification (larger plasma gasifier, CCGT, and CCS units), and these extra costs outweigh the modest savings from treating less food waste.

3.1.5. LCOE, LCObM, and LCOWT uncertainty analysis

An uncertainty analysis was conducted to evaluate the effect of simultaneous variations in all the uncertainty parameters and to quantitatively determine the range of variability in the economic criteria. A Monte Carlo simulation, developed in the MATLAB environment, applies the economic model to assess the impact of the variables listed in Table 9 on the LCOE, LCObM and LCOWT. Each of these three costs was recalculated across 10,000 trials, which produces a probability distribution curve. From these curves, essential statistical metrics such as the mean, median, and standard deviation are determined. Furthermore, the probability range of the LCOE, LCObM and LCOWT is defined using the 95 % CI statistical metric.

Table 9 presents the results of the Monte Carlo simulation used to estimate the LCOE, LCObM and LCOWT. The mean values are higher than those estimated in the deterministic economic assessment, reflecting the impact of CAPEX uncertainty. As shown in Table 9, the LCOE has less variance than the LCObM. This means that the biomethane price may be more sensitive to economic uncertainties. In addition, Scenario 1 consistently has a higher LCOWT than Scenario 2 across all cases, suggesting that electricity-focused production incurs higher waste treatment costs than biomethane-focused production. This is reasonable, as the PEC of CCGT is the largest cost component, meaning the higher electricity production capacity in Scenario 1 results in greater CAPEX which ultimately raises waste treatment costs compared to Scenario 2.

3.1.6. Economies of scale

The economies of scale for the proposed plant were assessed by varying the plant size between 100 MW_{th} to 750 MW_{th} of feedstock on

Table 9
Monte Carlo simulation results for estimating the LCOE, LCObM, and LCOWT.

Scenario	Case	Metric	Mean	Median	STD	95 % CI	Units
1	1	LCOE	0.1761	0.1749	0.0249	0.127 to 0.225	USD/kWh of electricity
	2	LCOE	0.3195	0.3184	0.0366	0.248 to 0.391	
	3	LCOE	0.3647	0.3635	0.0417	0.283 to 0.446	
2	1	LCObM	0.1839	0.1819	0.0419	0.102 to 0.266	USD/kWh of liquid biomethane
	2	LCObM	0.3323	0.3306	0.0416	0.251 to 0.414	
	3	LCObM	0.3864	0.3850	0.0530	0.285 to 0.490	
1	1	LCOWT	0.0893	0.0878	0.0312	0.028 to 0.150	USD/kg of waste
	2	LCOWT	0.1910	0.1900	0.0325	0.127 to 0.255	
	3	LCOWT	0.2459	0.2448	0.0395	0.168 to 0.323	
2	1	LCOWT	0.0854	0.0841	0.0265	0.033 to 0.137	
	2	LCOWT	0.1797	0.1786	0.0263	0.128 to 0.231	
	3	LCOWT	0.2151	0.2143	0.0333	0.150 to 0.280	

Note: case 1: baseline case; case 2: with pre-CCS case; case 3: with post-CCS case.

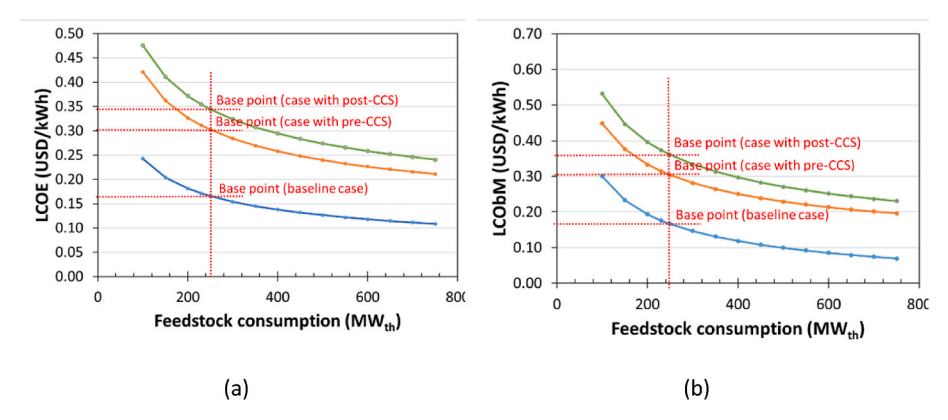


Fig. 11. Economies of scale for the investigated scenarios: (a) Scenario 1 and (b) Scenario 2.

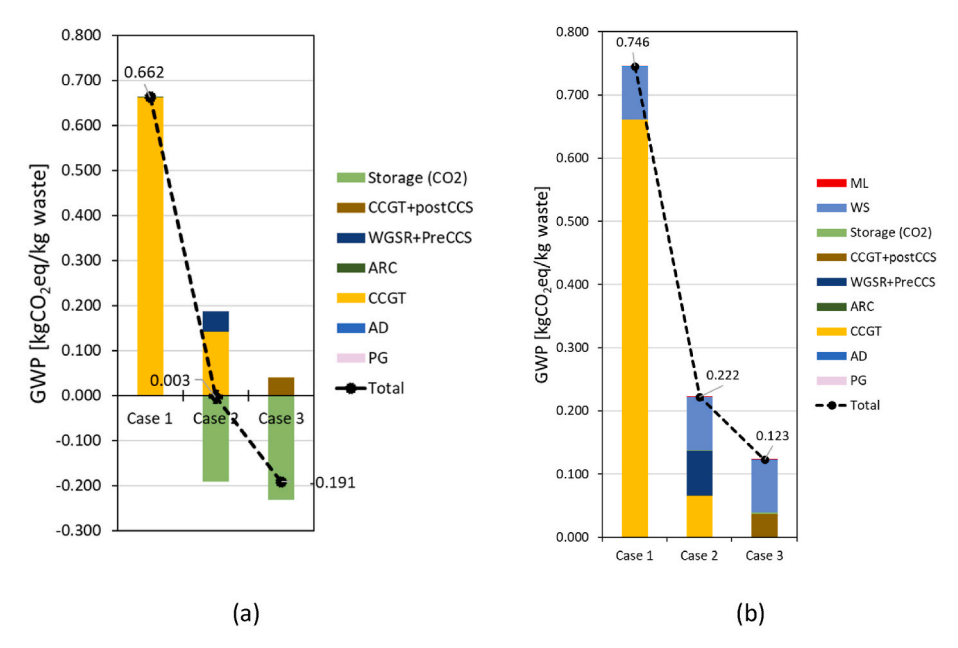


Fig. 12. The breakdown of the GWP under (a) Scenario 1 and (b) Scenario 2 (Note: case 1: baseline case; case 2: with pre-CCS case; case 3: with post-CCS case).

the LCOE and LCObM. CAPEX was adjusted using component-specific scaling factors (f), as outlined in Table 4. Fixed OPEX components were scaled proportionally to CAPEX. Although labor costs were calculated based on the number of system components rather than plant capacity (Equation (1), Supplementary Information (Alkhayat and Gerrard, 1984)), they were assumed to scale with plant capacity to the power of 0.242 to account for economies of scale, following the labor cost correlation proposed by Peters et al. (Peters and Timmerhaus, 1991).

Fig. 11a–b illustrate the relationship between feedstock consumption and the corresponding LCOE and LCObM, respectively. Both figures demonstrate that as the feedstock consumption increases, the associated LCOE and LCObM decrease. In Scenario 1, for feedstock input levels between 100 MWth and 200 MWth, the LCOE declines significantly. Specifically, the LCOE decreases from 0.24 to 0.18 USD/kWh for Case 1, from 0.42 to 0.33 USD/kWh for Case 2, and from 0.48 to 0.37 USD/kWh for Case 3. Beyond 250 MWth, the rate of decline slows considerably, with values reaching 0.11 USD/kWh for Case 1, 0.21 USD/kWh for Case 2, and 0.24 USD/kWh for Case 3 at a feedstock consumption level of 750 MWth.

In Scenario 2, a similar trend is observed. For feedstock input levels between 100 MW $_{th}$ and 200 MW $_{th}$, the LCObM decreases sharply, from 0.30 to 0.19 USD/kWh for Case 1, from 0.45 to 0.33 USD/kWh for Case 2, and from 0.53 to 0.40 USD/kWh for Case 3. Beyond 250 MW $_{th}$, the

reduction rate slows significantly, with values stabilizing at 0.07 USD/kWh for Case 1, 0.20 USD/kWh for Case 2, and 0.23 USD/kWh for Case 3 at 750 $\rm MW_{th}.$

While economies of scale provide initial cost reductions, further scaling beyond $600~\text{MW}_{\text{th}}$ of feedstock consumption yields diminishing economic benefits, as indicated by the flattening of the curves.

3.2. Environmental performance

The LCI data were processed using the SimaPro software to quantify the contributions to various midpoint impact categories. The developed inventory based on the mass and energy balance which has been normalized on a basis of 1 kg of waste can be seen in the **Supplementary Information** Section S.4. The LCA is performed by evaluating the input and output flows within the system boundary illustrated in Fig. 1, without modelling the internal processes.

In this section, GWP and water footprint (WF) are discussed as the key midpoint indicators. Additional impact indicators are available in the **Supplementary Information** Section S.5. All impact category results are normalized to 1 kg of waste processed within the system.

3.2.1. GWP

Fig. 12a-b presents the GWP impact breakdown for the different process stages in Scenario 1 and Scenario 2, respectively. As shown in

the figures, the baseline case in both scenarios exhibits the highest GWP, with Scenario 1 reaching approximately 0.662 kgCO2-eq/kg waste and Scenario 2 reaching 0.746 kgCO₂-eq/kg waste. The slightly lower GWP in the baseline case of Scenario 1 compared to Scenario 2 results from the off-gas emitted from the water scrubber, which is used for upgrading biogas by removing CO2 and H2S (Cozma et al., 2015). The stripper of the water scrubber releases off-gas composed of CO₂ (17.9 %), CH₄ (0.43 %), NH₃ (1 %), H₂S (0.16 %), O₂ (14.8 %), and N₂ (64 %), with all carbon emissions being biogenic. While biogenic CO2 emissions are excluded from the GWP calculation as carbon-neutral, biogenic methane emissions contribute significantly to the GWP. According to the ReCiPe 2016 method (Huijbregts et al., 2017) and supported by the SimaPro database, biogenic methane is assigned a GWP of approximately 33.25 kg CO₂-eq/kg CH₄. Consequently, the baseline case in Scenario 2 exhibits a slightly higher GWP compared to Scenario 1 due to the biogenic methane released from the water scrubber.

Compared to the literature, the GWP in the baseline case is higher than the GWP reported in a waste-to-heat-and-power system utilizing an incinerator without CCS, where the GWP was approximately 0.425 kg $\rm CO_2$ -eq/kg waste (Materazzi et al., 2024). The difference is primarily attributed to the higher proportion of biogenic carbon in the feedstock used in the reference study compared to the present study. The feedstock in the reference study contained approximately 64 % biogenic carbon, whereas in the current study, the proportion of biogenic carbon is significantly lower, at only 28 %.

For cases incorporating CCS, the pre-CCS configuration resulted in a higher GWP than the post-CCS configuration in both scenarios. Specifically, the GWP values for the pre-CCS case are 0.004 kgCO₂-eq/kg waste and 0.222 kgCO₂-eq/kg waste in Scenarios 1 and 2, respectively. In contrast, the post-CCS case achieved lower GWP values of $-0.191\,$ kgCO₂-eq/kg waste for Scenario 1 and 0.123 kgCO₂-eq/kg waste for Scenario 2. The higher GWP in the pre-CCS case compared to the post-CCS case is primarily due to the direct release of flue gas emissions from the combustion process in the CCGT, as these emissions are not treated or captured. Conversely, in the post-CCS case, a significant amount of CO₂ emissions is captured, reducing the overall GWP.

Additionally, the lower GWP in both the pre-CCS and post-CCS cases of Scenario 1 is attributed to the presence of biogenic carbon in the captured CO_2 , whereas in Scenario 2, the captured CO_2 is entirely of fossil origin. A previous study (Materazzi et al., 2024) reported a lower GWP of -0.416 kgCO₂-eq/kg waste in the incinerator integrated with the CCS, which is lower than the values obtained in this study. This discrepancy is primarily due to a higher proportion of biogenic carbon

sequestration in the reference study.

As shown in Fig. 12, the CCGT operation is the primary contributor to GWP in all cases due to the release of fossil and biogenic carbon emissions in Scenario 1 and fossil carbon emissions in Scenario 2. The fossil carbon emissions originate from plastic waste, while biogenic carbon emissions stem from food waste. In Fig. 12a, the implementation of pre-CCS reduces CCGT emissions from 0.661 kgCO2-eq/kg waste to 0.141 kgCO₂-eq/kg waste, while post-CCS integration further decreases emissions to -0.0392 kgCO₂-eq/kg waste. Similarly, Fig. 12b, which illustrates the GWP breakdown for Scenario 2, confirms that the operation of CCGT plant remains the dominant emission source. With pre-CCS, CCGT emissions decline from 0.661 kgCO₂-eq/kg waste to 0.066 kgCO₂-eq/kg waste, and with post-CCS, emissions are further reduced to 0.0369 kgCO₂-eq/kg waste. For a more detailed illustration of carbon emissions and their distribution throughout the process in all cases, Supplementary Information Section S.6 includes the diagram of the carbon molar flow.

3.2.2. WF

Fig. 13a–b illustrate the WF in Scenario 1 and Scenario 2, respectively. Among all cases, the pre-CCS case exhibits the highest WF, reaching approximately $0.0014~\text{m}^3/\text{kg}$ waste in Scenario 1 and $0.0013~\text{m}^3/\text{kg}$ waste in Scenario 2. This is primarily due to the substantial amount of water required for steam generation to support the operation of WGSR. Meanwhile, the post-CCS case exhibits the lowest WF, with values of $0.0010~\text{m}^3/\text{kg}$ waste for both scenarios.

Compared with literature reports on incineration-CCS integration for CHP (Materazzi et al., 2024), where WF values of up to $0.0234~\text{m}^3/\text{kg}$ waste have been observed, our results are markedly lower, likely because on-site wastewater treatment has been incorporated into the present study. Biogas production from energy crops (e.g., maize, sorghum, wheat) typically entails even higher WFs, ranging from 0.025~to $0.217~\text{m}^3/\text{kg}$ of crop (Pacetti et al., 2015). This disparity is attributed primarily to differences in feedstock moisture content: low-moisture energy crops demand substantially more water for anaerobic digestion than high-moisture food waste.

In both the baseline and post-CCS configurations, the CCGT constitutes the predominant contributor to the overall WF, accounting for over 50 % of the total in each case. The baseline WF is lower than that of the post-CCS configuration owing to the absence of LP steam diversion for stripper heating; consequently, all LP steam must be condensed, thereby requiring greater cooling-water consumption.

By contrast, in the pre-CCS configuration, the WF is dominated by

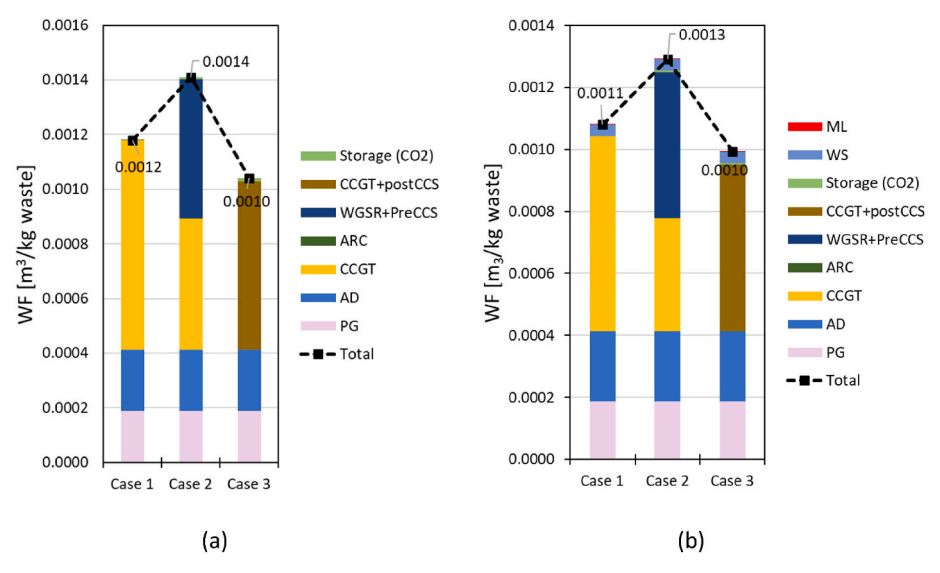


Fig. 13. The breakdown of the WF under (a) Scenario 1 and (b) Scenario 2 (Note: case 1: baseline case; case 2: with pre-CCS case; case 3: with post-CCS case).

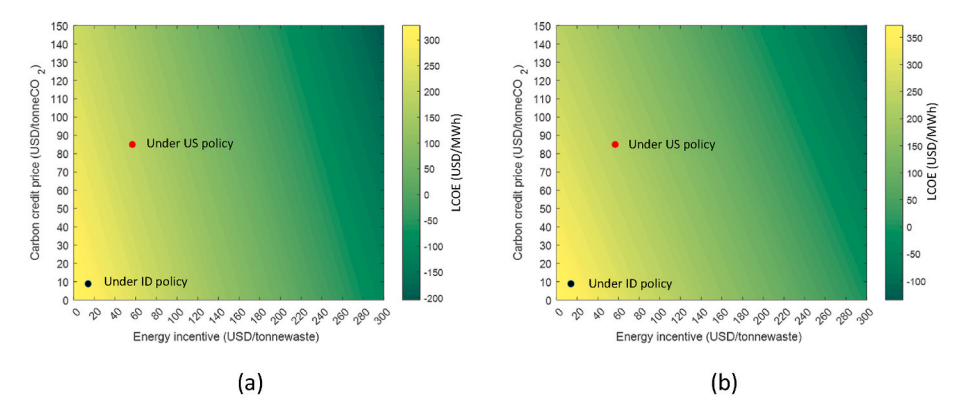


Fig. 14. Impact of carbon credit price and energy incentive on LCOE for different CCS configurations (a) pre-CCS and (b) post-CCS.

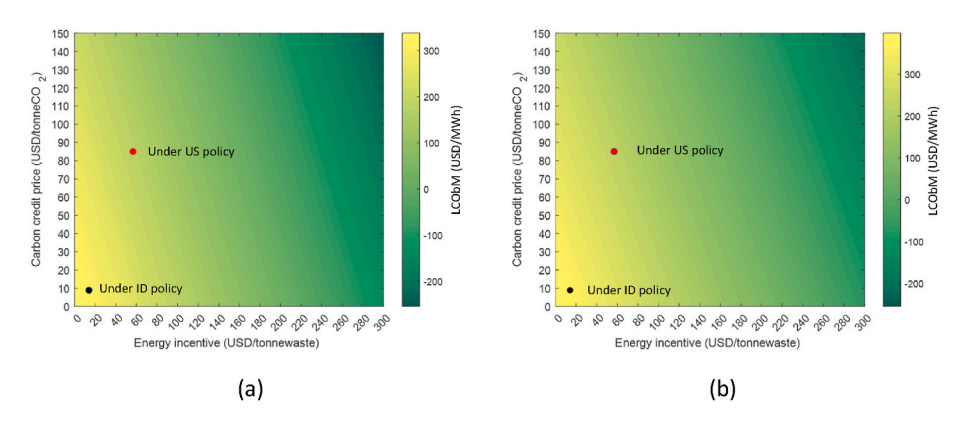


Fig. 15. Impact of carbon credit price and energy incentive on LCObM for different CCS configurations (a) pre-CCS and (b) post-CCS.

the water required for steam generation in the WGSR and pre-CCS units (denoted "WGSR + Pre-CCS" in the diagram), which together represent approximately 36 % of total WF in both scenarios. The CCGT contributes the next largest share, approximately 33 % in Scenario 1 and 28 % in Scenario 2. This reduced share reflects lower cooling-water demand for LP steam condensation, since 10 % of syngas is diverted to produce steam for the WGSR rather than for power generation, resulting in reduced fuel use and cooler condenser loads compared to the baseline and post-CCS cases.

3.2.3. Policy incentives analysis

This section examines the impact of waste utilization incentives and carbon credit pricing on the economic feasibility of the proposed WtE system. Figs. 14 and 15 illustrate the effect of employing potential policy schemes on the LCOE and LCObM, respectively. As shown, increasing energy incentives and carbon credit prices leads to a reduction in LCOE and LCObM, though the impact varies between the two configurations. The post-CCS case exhibits a higher LCOE and LCObM range than the pre-CCS due to the higher CAPEX and OPEX associated with the larger size of the CCGT and the additional costs of post-combustion $\rm CO_2$ capture and processing.

Indonesia has established a carbon credit price of $8.9~\mathrm{USD/tonne}$ CO₂ (Revanda, 2025) and provides financial incentives for waste utilization through tipping fees, which vary by municipality. In the city where the proposed system is located, the tipping fee reaches $14.02~\mathrm{USD/tonne}$ of waste (Erfinanto, 2024). Despite the application of both carbon credits and tipping fees, the reduction in LCOE is only 7.95~% for the pre-CCS case and 6.81~% for the post-CCS case. Similarly, the LCObM reduction is limited to 8.60~% and 7.65~% for pre-CCS and post-CCS configurations, respectively. Under Presidential Regulation No. $112~\mathrm{of}~2022~\mathrm{on}$ the Acceleration of Renewable Energy Development for Electricity Supply, the Indonesian government set the maximum electricity purchase price

for WtE plants with a capacity above 10 MW at USD 92.9/MWh for the first 10 years, decreasing to USD 59.44/MWh for years 11–25. Given that the LCOE of the current system far exceeds these limits, the project is not financially viable under existing policies.

To assess the potential impact of higher financial incentives, the carbon credit price and tipping fee values from the United States (U.S.) were applied as a benchmark. It is recognized that economic conditions in Indonesia differ markedly from those in the U.S., however, U.S. market data were selected as conservative, high-integrity proxies for two reasons. First, the U.S. carbon-credit market, both compliance and voluntary, is among the most developed globally. Robust regulatory frameworks for greenhouse-gas reductions have been established by state and regional cap-and-trade programs (e.g., California Air Resources Board, Oregon Clean Fuels Program, and the Regional Greenhouse Gas Initiative), and rigorous certification and registry systems for offset projects worldwide are maintained by leading voluntary standards bodies (Verra, Gold Standard, and the American Carbon Registry) (Sapkota and White, 2020). These combined mechanisms ensure transparent pricing, third-party verification, and publicly accessible transaction data, justifying the adoption of the U.S. carbon credit price of USD 85.00/tonne CO2 as an upper-bound benchmark (U.S. Department of Energy, 2025).

Second, the Environmental Research & Education Foundation's May 2024 survey of U.S. municipal landfills has been adopted, reporting an unweighted national average tipping fee of USD 56.80 per tonne (Environmental Research & Education Foundation (EREF), 2024). This fee is understood to fully internalize capital, operating, and long-term environmental compliance costs, and is therefore presented as a "best-practice" benchmark for cost-recovery assumptions. Under these U.S. benchmark conditions, the reductions in LCOE and LCObM due to the application of both carbon credits and tipping fees are substantial, ranging from 39 % to 47 %, demonstrating the potential for enhanced

financial viability with stronger policy support.

4. Conclusion

This study presents a novel WtE system integrating plastic waste plasma gasification and food waste anaerobic digestion for the production of CCHP, and liquid biomethane. While plasma gasification has primarily been applied for hydrogen production, its integration with CCS remains underexplored, particularly for plastic waste feedstocks and hybrid waste conversion processes such as anaerobic digestion. This study provides a cradle-to-gate assessment of multiple energy outputs, incorporating heat integration strategies to holistically evaluate economic and environmental performance. Several configurations were evaluated, and the key findings are summarized as follows:

- In Scenario 1, the LCOE spans from 0.171 to 0.354 USD/kWh, while
 in Scenario 2, the LCObM ranges between 0.176 and 0.374 USD/
 kWh. In both scenarios, the baseline case achieves the lowest levelized cost, whereas the case with post-CCS exhibits the highest
 levelized cost. This outcome reflects that the integration of a CCS
 plant increases both LCOE and LCObM.
- 2. In both scenarios, LCOWT falls between 0.081 and 0.236 USD/kg waste. The LCOWT in Scenario 1 is slightly higher than in Scenario 2, primarily due to the significantly higher CAPEX in Scenario 1.
- 3. Based on the sensitivity analysis, PEC of gas turbine power plant has the greatest impact on LCOE, LCObM, and LCOWT. Lowering this cost yields the largest reductions across all three metrics, highlighting its critical role in the system's economic feasibility.
- 4. Monte Carlo simulations reveal greater variability in LCObM compared to LCOE, with wider 95 % CI for LCObM which indicates that biomethane prices are more sensitive to economic uncertainties.
- 5. Scenario 1 exhibits GWP values between -0.191 and 0.662 kgCO₂-eq/kg waste, while Scenario 2 ranges from 0.123 to 0.746 kgCO₂-eq/kg waste, with post-CCS configurations yielding the lowest GWP, and the operation of CCGT being the largest GWP contributor across all cases due to the carbon emission.
- 6. Both scenarios exhibit WF values ranging from 0.0010 to $0.0014\,\mathrm{m}^3/\mathrm{kg}$ waste, with the CCGT as the primary contributor due to its high cooling water demand for LP steam condensation.
- 7. By applying Indonesia's policy incentives (both tipping fee and carbon credit), the LCOE and LCObM for the system with a CCS plant are reduced by less than 9 % which reflects a limited financial impact on improving the system's economic feasibility.

This research offers new insights into the design and performance of hybrid, low-emission WtE systems which illustrates the technical feasibility and trade-offs involved in coupling plasma gasification, anaerobic digestion, and CCS. The novel system design contributes to advancing the state-of-the-art in sustainable waste management and supports decision-making for both technology developers and policymakers. Future research can focus on developing a pilot-scale demonstration to validate the system's technical performance, economic feasibility, and environmental impact under real-world conditions.

CRediT authorship contribution statement

Qurrotin Ayunina Maulida Okta Arifianti: Writing – original draft, Validation, Software, Methodology, Investigation, Formal analysis, Conceptualization. Maria Fernanda Rojas Michaga: Writing – review & editing, Validation, Software, Methodology, Investigation. Karim Rabea: Writing – review & editing, Validation, Software, Methodology, Investigation. Stavros Michailos: Writing – review & editing, Software, Conceptualization. Kevin J. Hughes: Supervision, Software, Resources. Lin Ma: Supervision, Resources. Derek Ingham: Writing – review & editing, Resources. Mohamed Pourkashanian: Supervision, Resources, Project administration.

Declaration of competing interest

The authors declare that they have no known competing financial interests or personal relationships that could have appeared to influence the work reported in this paper.

Acknowledgement

This research was funded by the Indonesian Education Scholarship (BPI), Center for Higher Education Funding and Assessment (PPAPT), and Indonesian Endowment Fund for Education (LPDP). SM (fourth author) would like to acknowledge that this work was supported by the UKRI ISCF Industrial Decarbonisation Challenge, through the UK Industrial Decarbonisation Research and Innovation Centre (IDRIC) award number: EP/V027050/1, under the Industrial Decarbonisation Challenge (IDC) and the Engineering and Physical Sciences Research Council (EPSRC) under the United Kingdom CCS Research Centre grants EP/W002841/1. We also extend our gratitude to the University of Sheffield Institutional Open Access Fund for supporting the publication costs. For the purpose of open access, the author has applied a Creative Commons Attribution (CC BY) licence to any Author Accepted Manuscript version arising.

Appendix A. Supplementary data

Supplementary data to this article can be found online at $\frac{\text{https:}}{\text{doi.}}$ org/10.1016/j.cesys.2025.100324.

Data availability

Data will be made available on request.

References

- Aich, W., et al., 2024. Techno-economic and life cycle analysis of two different hydrogen production processes from excavated waste under plasma gasification. Process Saf. Environ. Prot. 184, 1158–1176. https://doi.org/10.1016/j.psep.2024.02.055.
- Akbarian, A., Andooz, A., Kowsari, E., Ramakrishna, S., Asgari, S., Cheshmeh, Z.A., 2022. Challenges and opportunities of lignocellulosic biomass gasification in the path of circular bioeconomy. Bioresour. Technol. 362, 127774.
- Albrecht, F.G., König, D.H., Baucks, N., Dietrich, R.-U., 2017. A standardized methodology for the techno-economic evaluation of alternative fuels – a case study. Fuel 194, 511–526. https://doi.org/10.1016/j.fuel.2016.12.003.
- Alelyani, S.M., Fette, N.W., Stechel, E.B., Doron, P., Phelan, P.E., 2017. Techno-economic analysis of combined ammonia-water absorption refrigeration and desalination. Energy Convers. Manag. 143, 493–504. https://doi.org/10.1016/j. enconman.2017.03.085.
- Alkhayat, W., Gerrard, A., 1984. Estimating manning levels for process plants. AACE
 Transactions 1
- Anaya-Reza, O., Altamirano-Corona, M.F., Castelán-Rodríguez, G., García-González, S.A., Durán-Moreno, A., 2022. Techno-economic and environmental assessment for biomethane production and cogeneration scenarios from OFMSW in Mexico. Waste Biomass Valor 13 (2), 1059–1075. https://doi.org/10.1007/s12649-021-01592-x.
- Antoniou, N., Monlau, F., Sambusiti, C., Ficara, E., Barakat, A., Zabaniotou, A., 2019. Contribution to circular economy options of mixed agricultural wastes management: coupling anaerobic digestion with gasification for enhanced energy and material recovery. J. Clean. Prod. 209, 505–514. https://doi.org/10.1016/j.jclepro.2018.10.055.
- Arena, U., Di Gregorio, F., Amorese, C., Mastellone, M.L., 2011. A techno-economic comparison of fluidized bed gasification of two mixed plastic wastes. Waste Manag. 31 (7), 1494–1504. https://doi.org/10.1016/j.wasman.2011.02.004.
- Arifianti, Q.A.M.O., et al., 2025. Conceptual design and thermodynamic investigation of novel energy and fuel generation systems from municipal waste coupled with carbon capture and storage. Energy Nexus, 100460.
- Bates, J., et al., 2005. Cost estimate classification System–As applied in engineering, procurement, and construction for the process industries. AACE International Recommended Practice 18.
- Bhering Trindade, A., Luiza Grillo Renó, M., José Rúa Orozco, D., Martín Martinez Reyes, A., Aparecido Vitoriano Julio, A., Carlos Escobar Palacio, J., 2021. Comparative analysis of different cost allocation methodologies in LCA for cogeneration systems. Energy Convers. Manag. 241, 114230. https://doi.org/ 10.1016/j.enconman.2021.114230.
- Brahme, R., Krishnan, P., Tiwari, K., 2023. 'Economics of waste management'. In: 360-Degree Waste Management, vol. 1. Elsevier, pp. 239–264. https://doi.org/10.1016/B978-0-323-90760-6.00002-3.

- Calvin, K., et al., 2023. IPCC, 2023: climate change 2023: synthesis report. In: Lee, H., Romero, J. (Eds.), Contribution of Working Groups I, II and III to the Sixth Assessment Report of the Intergovernmental Panel on Climate Change [Core Writing Team. Intergovernmental Panel on Climate Change (IPCC), Geneva, Switzerland. https://doi.org/10.59327/IPCC/AR6-9789291691647. IPCC.
- Capital cost estimating. In: Chemical Engineering Design, 2013. Elsevier, pp. 307–354. https://doi.org/10.1016/b978-0-08-096659-5.00007-9.
- Capra, F., Magli, F., Gatti, M., 2019. Biomethane liquefaction: a systematic comparative analysis of refrigeration technologies. Appl. Therm. Eng. 158, 113815. https://doi. org/10.1016/j.applthermaleng.2019.113815.
- Chari, S., Sebastiani, A., Paulillo, A., Materazzi, M., 2023. The environmental performance of mixed plastic waste gasification with carbon capture and storage to produce hydrogen in the U.K. ACS Sustainable Chem. Eng. 11 (8), 3248–3259. https://doi.org/10.1021/acssuschemeng.2c05978.
- Chen, J., et al., 2019. Thermodynamic and environmental analysis of integrated supercritical water gasification of coal for power and hydrogen production. Energy Convers. Manag. 198, 111927. https://doi.org/10.1016/j.enconman.2019.111927.
- Chen, H., et al., 2022. Performance assessment of a novel medical-waste-to-energy design based on plasma gasification and integrated with a municipal solid waste incineration plant. Energy 245, 123156. https://doi.org/10.1016/j.energy.2022.123156.
- Cho, I.J., Park, H.-W., Park, D.-W., Choi, S., 2015. Enhancement of synthesis gas production using gasification-plasma hybrid system. Int. J. Hydrogen Energy 40 (4), 1709–1716.
- Choi, S., Kim, S., Jung, M., Lee, J., Lim, J., Kim, M., 2022. Comparative analysis of exergy- and enthalpy-based allocation methods for cogeneration businesses in the industrial complex of South Korea. Energy 240, 122837. https://doi.org/10.1016/j. energy.2021.122837.
- Coppitters, D., De Paepe, W., Contino, F., 2021. Robust design optimization of a photovoltaic-battery-heat pump system with thermal storage under aleatory and epistemic uncertainty. Energy 229, 120692. https://doi.org/10.1016/j. energy.2021.120692.
- Cozma, P., Wukovits, W., Mămăligă, I., Friedl, A., Gavrilescu, M., 2015. Modeling and simulation of high pressure water scrubbing technology applied for biogas upgrading. Clean Technol. Environ. Policy 17 (2), 373–391. https://doi.org/ 10.1007/s10098-014-0787-7.
- Cudjoe, D., Wang, H., 2022. Plasma gasification versus incineration of plastic waste: energy, economic and environmental analysis. Fuel Process. Technol. 237, 107470. https://doi.org/10.1016/j.fuproc.2022.107470.
- Cudjoe, D., Zhu, B., 2024. Gasification of medical plastic waste into hydrogen: energy potential, environmental benefits and economic feasibility. Fuel 371, 132150. https://doi.org/10.1016/j.fuel.2024.132150.
- Cuéllar-Franca, R., García-Gutiérrez, P., Dimitriou, I., Elder, R.H., Allen, R.W.K., Azapagic, A., 2019. Utilising carbon dioxide for transport fuels: the economic and environmental sustainability of different fischer-tropsch process designs. Appl. Energy 253, 113560. https://doi.org/10.1016/j.apenergy.2019.113560.
- DECC, 2016. Electricity Generation Costs and Hurdle Rates for Non-renewable Technologies. Electricity Generation Costs and Hurdle Rates' [Online]. Available: https://assets.publishing.service.gov.uk/government/uploads/system/uploads/a ttachment data/file/566803/Leigh_Fisher_Non-renewable_Generation_Cost.pdf.
- Díaz-Ramírez, M., Jokull, S., Zuffi, C., Mainar-Toledo, M.D., Manfrida, G., 2023. Environmental assessment of hellisheidi geothermal power plant based on exergy allocation factors for heat and electricity production. Energies 16 (9), 3616. https://doi.org/10.3390/en16093616.
- Dimitriou, I., Goldingay, H., Bridgwater, A.V., 2018. Techno-economic and uncertainty analysis of biomass to liquid (BTL) systems for transport fuel production. Renew. Sustain. Energy Rev. 88, 160–175. https://doi.org/10.1016/j.rser.2018.02.023.
- Ekvall, T., Finnveden, G., 2001. Allocation in ISO 14041—a critical review. J. Clean. Prod. 9 (3), 197–208. https://doi.org/10.1016/S0959-6526(00)00052-4.
- Environmental Research & Education Foundation (EREF), 2024. Analysis of MSW Landfill Tipping Fees — 2023. Environmental Research & Education Foundation (EREF) [Online]. Available: www.erefdn.org. (Accessed 6 August 2025).
- Fernanda Rojas Michaga, M., et al., 2022. Bioenergy with carbon capture and storage (BECCS) potential in jet fuel production from forestry residues: a combined technoeconomic and life cycle assessment approach. Energy Convers. Manag. 255, 115346. https://doi.org/10.1016/j.enconman.2022.115346.
- Fridman, A., 2008. Plasma Chemistry. Cambridge university press.
- Gabbar, H.A., Lisi, D., Aboughaly, M., Damideh, V., Hassen, I., 2020. Modeling of a plasma-based waste gasification system for solid waste generated onboard of typical cruiser vessels used as a feedstock. Designs 4 (3), 33. https://doi.org/10.3390/ designs.0030033
- Galaly, A.R., Dawood, N., 2023. Energy recovery and economic evaluation for industrial fuel from plastic waste. Polymers 15 (11), 2433. https://doi.org/10.3390/ polymi5112432
- Ghiat, I., AlNouss, A., McKay, G., Al-Ansari, T., 2020. Biomass-based integrated gasification combined cycle with post-combustion CO2 recovery by potassium carbonate: techno-Economic and environmental analysis. Comput. Chem. Eng. 135, 106758. https://doi.org/10.1016/j.compchemeng.2020.106758.
- Hadidi, L.A., Omer, M.M., 2017. A financial feasibility model of gasification and anaerobic digestion waste-to-energy (WTE) plants in Saudi Arabia. Waste Manag. 59, 90–101. https://doi.org/10.1016/j.wasman.2016.09.030.
- Han, Y., Sun, Y., 2020. Collaborative optimization of energy conversion and NOx removal in boiler cold-end of coal-fired power plants based on waste heat recovery of flue gas and sensible heat utilization of extraction steam. Energy 207, 118172. https://doi.org/10.1016/j.energy.2020.118172.

- Huijbregts, M.A.J., et al., 2017. ReCiPe2016: a harmonised life cycle impact assessment method at midpoint and endpoint level. Int. J. Life Cycle Assess. 22 (2), 138–147. https://doi.org/10.1007/s11367-016-1246-y.
- Index Mundi, 2023. [Online]. Available: https://www.indexmundi.com/commodities/? commodity=indonesian-liquified-natural-gas&months=120. (Accessed 14 January 2025).
- International Energy Agency, 2023. Net Zero Roadmap A Global Pathway to Keep the 1.5 °C Goal in Reach. International Energy Agency [Online]. Available: https://www.iea.org/reports/net-zero-roadmap-a-global-pathway-to-keep-the-15-0c-goal-in-reach.
- Jana, K., De, S., 2016. Environmental impact of an agro-waste based polygeneration without and with CO 2 storage: life cycle assessment approach. Bioresour. Technol. 216, 931–940. https://doi.org/10.1016/j.biortech.2016.06.039.
- Janajreh, I., Raza, S.S., Valmundsson, A.S., 2013. Plasma gasification process: modeling, simulation and comparison with conventional air gasification. Energy Convers. Manag. 65, 801–809. https://doi.org/10.1016/j.enconman.2012.03.010.
- Javed, M.H., Ahmad, A., Rehan, M., Musharavati, F., Nizami, A.-S., Khan, M.I., 2025. Advancing sustainable energy: environmental and economic assessment of plastic waste gasification for syngas and electricity generation using life cycle modeling. Sustainability 17 (3), 1277. https://doi.org/10.3390/su17031277.
- Jones, P.T., et al., 2013. Enhanced landfill mining in view of multiple resource recovery: a critical review. J. Clean. Prod. 55, 45–55. https://doi.org/10.1016/j. iclepro.2012.05.021.
- Jouhara, H., Khordehgah, N., Almahmoud, S., Delpech, B., Chauhan, A., Tassou, S.A., 2018. Waste heat recovery technologies and applications. Therm. Sci. Eng. Prog. 6, 268–289. https://doi.org/10.1016/j.tsep.2018.04.017.
- Lan, K., Yao, Y., 2022. Feasibility of gasifying mixed plastic waste for hydrogen production and carbon capture and storage. Commun. Earth Environ. 3 (1), 300. https://doi.org/10.1038/s43247-022-00632-1.
- Lebreton, L., Andrady, A., 2019. Future scenarios of global plastic waste generation and disposal. Palgrave Commun 5 (1), 6. https://doi.org/10.1057/s41599-018-0212-7.
- Li, Y., Han, Y., Zhang, Y., Luo, W., Li, G., 2020. Anaerobic digestion of different agricultural wastes: a techno-economic assessment. Bioresour. Technol. 315, 123836. https://doi.org/10.1016/j.biortech.2020.123836.
- Li, J., et al., 2023. Comparative thermodynamic and techno-economic analysis of various medical waste-to-hydrogen/methanol pathways based on plasma gasification. Appl. Therm. Eng. 221, 119762. https://doi.org/10.1016/j.applthermaleng.2022.119762.
- Erfinanto, E., 2024. 'DPRD surabaya usulkan pembangunan tempat pembuangan sampah baru, TPA benowo penuh', liputan 6 [Online]. Available: https://www.liputan6.com/surabaya/read/5583317/dprd-surabaya-usulkan-pembangunan-tempat-pembuangan-sampah-baru-tpa-benowo-penuh. (Accessed 3 February 2025).
- Limanseto, H., 2025. Mendorong Implementasi Teknologi Carbon Capture and Storage (CCS) untuk Pertumbuhan Ekonomi Berkelanjutan di Indonesia', Kementerian Koordinator Bidang Perekonomian. Press Release HM.02.04/75/SET.M.EKON.3/02/ 2025 [Online]. Available: https://ekon.go.id/publikasi/detail/6226/mendorong-implementasi-teknologi-carbon-capture-and-storage-ccs-untuk-pertumbuhan-ekonomi-berkelanjutan-di-indonesia. (Accessed 10 March 2025).
- Lin, L., Shah, A., Keener, H., Li, Y., 2019. Techno-economic analyses of solid-state anaerobic digestion and composting of yard trimmings. Waste Manag. 85, 405–416. https://doi.org/10.1016/j.wasman.2018.12.037
- https://doi.org/10.1016/j.wasman.2018.12.037.
 Mallick, R., Prabu, V., 2022. 4-E analyses of plasma gasification integrated chemical looping reforming system for power and hydrogen co-generation using bakelite and acrylonitrile butadiene styrene based plastic waste feedstocks. Energy Convers. Manag. 271, 116320. https://doi.org/10.1016/j.enconman.2022.116320.
- Mallick, R., Vairakannu, P., 2023. Experimental investigation of acrylonitrile butadiene styrene plastics plasma gasification. J. Environ. Manag. 345, 118655. https://doi. org/10.1016/j.jenyman.2023.118655.
- Materazzi, M., Chari, S., Sebastiani, A., Lettieri, P., Paulillo, A., 2024. Waste-to-energy and waste-to-hydrogen with CCS: methodological assessment of pathways to carbonnegative waste treatment from an LCA perspective. Waste Manag. 173, 184–199. https://doi.org/10.1016/j.wasman.2023.11.020.
- Michailos, S., Emenike, O., Ingham, D., Hughes, K.J., Pourkashanian, M., 2019. Methane production via syngas fermentation within the bio-CCS concept: a techno-economic assessment. Biochem. Eng. J. 150, 107290. https://doi.org/10.1016/j. bei.2019.107290.
- Michailos, S., Walker, M., Moody, A., Poggio, D., Pourkashanian, M., 2020. Biomethane production using an integrated anaerobic digestion, gasification and CO2 biomethanation process in a real waste water treatment plant: a techno-economic assessment. Energy Convers. Manag. 209, 112663. https://doi.org/10.1016/j.enconman.2020.112663.
- Minutillo, M., Perna, A., Di Bona, D., 2009. Modelling and performance analysis of an integrated plasma gasification combined cycle (IPGCC) power plant. Energy Convers. Manag. 50 (11), 2837–2842. https://doi.org/10.1016/j.
- Montiel-Bohórquez, N.D., Saldarriaga-Loaiza, J.D., Pérez, J.F., 2021. A techno-economic assessment of syngas production by plasma gasification of municipal solid waste as a substitute gaseous fuel. J. Energy Resour. Technol. 143 (9), 090901. https://doi.org/ 10.1115/1.4049285.
- Montiel-Bohórquez, N.D., Saldarriaga-Loaiza, J.D., Pérez, J.F., 2022. Analysis of investment incentives for power generation based on an integrated plasma gasification combined cycle power plant using municipal solid waste. Case Stud. Therm. Eng. 30, 101748. https://doi.org/10.1016/j.csite.2021.101748.
- Mountouris, A., Voutsas, E., Tassios, D., 2006. Solid waste plasma gasification: equilibrium model development and exergy analysis. Energy Convers. Manag. 47 (13–14), 1723–1737. https://doi.org/10.1016/j.enconman.2005.10.015.

- Mullen, D., Lucquiaud, M., 2024. On the cost of zero carbon electricity: a technoeconomic analysis of combined cycle gas turbines with post-combustion CO2 capture. Energy Rep. 11, 5104–5124. https://doi.org/10.1016/j.egyr.2024.04.067.
- Nagar, V., Kaushal, R., 2024. A review of recent advancement in plasma gasification: a promising solution for waste management and energy production. Int. J. Hydrogen Energy 77, 405–419. https://doi.org/10.1016/j.ijhydene.2024.06.180.
- Oliveira, M., Ramos, A., Ismail, T.M., Monteiro, E., Rouboa, A., 2022. A review on plasma gasification of solid residues: recent advances and developments. Energies 15 (4), 1475.
- Onel, O., Niziolek, A.M., Elia, J.A., Baliban, R.C., Floudas, C.A., 2015. Biomass and natural gas to liquid transportation fuels and olefins (BGTL+C2_C4): process synthesis and global optimization. Ind. Eng. Chem. Res. 54 (1), 359–385. https://doi.org/10.1021/ie503979b.
- Pacetti, T., Lombardi, L., Federici, G., 2015. Water–energy nexus: a case of biogas production from energy crops evaluated by water footprint and life cycle assessment (LCA) methods. J. Clean. Prod. 101, 278–291. https://doi.org/10.1016/j. jclepro.2015.03.084.
- Peters, M.S., Timmerhaus, K.D., 1991. Plant design and economics for chemical engineers. In: McGraw-Hill Chemical Engineering Series, fourth ed. McGraw-Hill, New York
- Ratchawang, S., Chotpantarat, S., Chokchai, S., Takashima, I., Uchida, Y., Charusiri, P., 2022. A review of ground source heat pump application for space cooling in southeast Asia. Energies 15 (14), 4992. https://doi.org/10.3390/en15144992.
- Revanda, H., 2025. 'RI resmi Luncurkan perdagangan karbon internasional, harga Rp 96 ribu dan Rp 144 ribu per ton', tempo [Online]. Available: https://www.tempo.co/ekonomi/ri-resmi-luncurkan-perdagangan-karbon-internasional-harga-rp-96-ribu-dan-rp-144-ribu-per-ton-1196430. (Accessed 25 January 2025).
- Rida Galaly, A., Van Oost, G., Dawood, N., 2024. Sustainable plasma gasification treatment of plastic waste: evaluating environmental, economic, and strategic dimensions. ACS Omega 9 (19), 21174–21186. https://doi.org/10.1021/ acsomega 4c01084
- Rutberg, Ph G., Bratsev, A.N., Kuznetsov, V.A., Popov, V.E., Ufimtsev, A.A., Shtengel', S. V., 2011. On efficiency of plasma gasification of wood residues. Biomass Bioenergy 35 (1), 495–504. https://doi.org/10.1016/j.biombioe.2010.09.010.
- Rutberg, P.G., et al., 2013. Novel three-phase steam-air plasma torch for gasification of high-caloric waste. Appl. Energy 108, 505–514. https://doi.org/10.1016/j. apenergy.2013.03.052.
- Sapkota, Y., White, J.R., 2020. Carbon offset market methodologies applicable for coastal wetland restoration and conservation in the United States: a review. Sci. Total Environ. 701, 134497. https://doi.org/10.1016/j.scitotenv.2019.134497.
- Siahaan, M., 2025. 'average cost of electricity supply in Indonesia from 2014 to 2023', statista [Online]. Available: https://www.statista.com/statistics/994512/averag e-electricity-cost-indonesia/. (Accessed 25 November 2024).
- Soltani, S., 2019. Modified exergy and exergoeconomic analyses of a biomass post fired hydrogen production combined cycle. Renew. Energy 135, 1466–1480. https://doi. org/10.1016/j.renene.2018.09.074.
- Tang, J., et al., 2023. From excavated waste to hydrogen: life cycle technoenvironmental-economic comparison between plasma-gasification-based water gas shift and sorption enhanced water gas shift routes. Energy Convers. Manag. 292, 117375. https://doi.org/10.1016/i.enconman.2023.117375.

- United Nations: Department of Economic and Social Affairs, 2023. 'Sustainable Development Goals', THE 17 GOALS [Online]. Available: https://sdgs.un.org/goals. (Accessed 1 August 2025).
- United Nations Environment Programme and International Solid Waste Association, 2024. Global waste management outlook 2024 - beyond an age of waste: turning rubbish into a resource. United Nations Environment Programme. https://doi.org/ 10.59117/20.500.11822/44939.
- U.S. Department of Energy, 2025. Carbon negative shot [Online]. Available: https://www.energy.gov/topics/carbon-negative-shot. (Accessed 22 January 2025).
- Von Der Assen, N., Jung, J., Bardow, A., 2013. Life-cycle assessment of carbon dioxide capture and utilization: avoiding the pitfalls. Energy Environ. Sci. 6 (9), 2721. https://doi.org/10.1039/c3ee41151f.
- Wang, S., et al., 2021. Techno-economic-environmental evaluation of a combined cooling heating and power system for gas turbine waste heat recovery. Energy 231, 120956. https://doi.org/10.1016/j.energy.2021.120956.
- Wei, Y., et al., 2024. Evaluation of greenhouse gas emission and reduction potential of high-food-waste-content municipal solid waste landfills: a case study of a landfill in the east of China. Waste Manag. 189, 290–299. https://doi.org/10.1016/j. wasman.2024.08.029
- Xu, F., Li, Y., Ge, X., Yang, L., Li, Y., 2018. Anaerobic digestion of food waste challenges and opportunities. Bioresour. Technol. 247, 1047–1058. https://doi.org/10.1016/j. biortech.2017.09.020.
- Xu, W., et al., 2025. Comprehensive analysis and life cycle assessment of polygeneration systems based on plasma gasification and combined cycle power generation. ACS Sustainable Chem. Eng. https://doi.org/10.1021/acssuschemeng.4c09282 acssuschemeng.4c09282.
- Yang, F., Meerman, J.C., Faaij, A.P.C., 2021. Carbon capture and biomass in industry: a techno-economic analysis and comparison of negative emission options. Renew. Sustain. Energy Rev. 144, 111028. https://doi.org/10.1016/j.rser.2021.111028.
- Zang, G., Jia, J., Tejasvi, S., Ratner, A., Silva Lora, E., 2018. Techno-economic comparative analysis of biomass integrated gasification combined cycles with and without CO2 capture. Int. J. Greenh. Gas Control 78, 73–84. https://doi.org/ 10.1016/j.ijggc.2018.07.023.
- Zare, V., 2020. Role of modeling approach on the results of thermodynamic analysis: concept presentation via thermoeconomic comparison of biomass gasification-fueled open and closed cycle gas turbines. Energy Convers. Manag. 225, 113479. https:// doi.org/10.1016/j.enconman.2020.113479.
- Zhang, R., et al., 2007. Characterization of food waste as feedstock for anaerobic digestion. Bioresour. Technol. 98 (4), 929–935. https://doi.org/10.1016/j. biortech.2006.02.039.
- Zhang, J., et al., 2020. Integrating food waste sorting system with anaerobic digestion and gasification for hydrogen and methane co-production. Appl. Energy 257, 113988. https://doi.org/10.1016/j.apenergy.2019.113988.
- Zhao, Y., et al., 2023. Energy, efficiency, and environmental analysis of hydrogen generation via plasma co-gasification of biomass and plastics based on parameter simulation using aspen plus. Energy Convers. Manag. 295, 117623. https://doi.org/ 10.1016/j.encomman.2023.117623.
- Zhou, R., et al., 2023. Plasma-electrified up-carbonization for low-carbon clean energy. Carbon Energy 5 (1), e260.